



Cite this: *Chem. Soc. Rev.*, 2024, 53, 606

# Stimulus-responsive polymer materials toward multi-mode and multi-level information anti-counterfeiting: recent advances and future challenges

Ying Shen,<sup>ab</sup> Xiaoxia Le,<sup>id</sup> \*<sup>ab</sup> Yue Wu<sup>ab</sup> and Tao Chen<sup>id</sup> \*<sup>abc</sup>

Information storage and security is one of the perennial hot issues in society, while the further advancements of related chemical anti-counterfeiting systems remain a formidable challenge. As emerging anti-counterfeiting materials, stimulus-responsive polymers (SRPs) have attracted extensive attention due to their unique stimulus-responsiveness and charming discoloration performance. At the same time, single-channel decryption technology with low-security levels has been unable to effectively prevent information from being stolen or mimicked. As a result, it would be of great significance to develop SRPs with multi-mode and multi-level anti-counterfeiting characteristics. This study summarizes the latest achievements in advance anti-counterfeiting strategies based on SRPs, including multi-mode anti-counterfeiting (static information) and multi-level anti-counterfeiting (dynamic information). In addition, the promising applications of such materials in anti-counterfeiting labels, identification platforms, intelligent displays, and others are briefly reviewed. Finally, the challenges and opportunities in this emerging field are discussed. This review serves as a useful resource for manipulating SRP-based anti-counterfeiting materials and creating cutting-edge information security and encryption systems.

Received 11th September 2023

DOI: 10.1039/d3cs00753g

rsc.li/chem-soc-rev

## Key learning points

- (1) The general concept of stimulus-responsive polymer (SRP)-based information-storage materials, devices, and their significance in the field of information security.
- (2) The methods used to construct SRPs with multi-mode and multi-level anti-counterfeiting performance.
- (3) The working mechanisms of SRP-based information-storage materials, devices, and the corresponding encryption-decryption techniques.
- (4) The elaboration of SRP-based information storage-devices with multiple synergistic functions that display multi-mode or multi-level anti-counterfeiting.
- (5) The challenges that such SRP-based information-storage devices encounter and the prospects for their future development.

## 1. Introduction

With the booming of modern technology, the issues of counterfeiting and shoddy goods are spreading over the global markets, posing serious threats to product identification, human health, and even national security. Simultaneously, corresponding

information security problems are also continuously emerging, including the leakage of confidential documents, breach of information integrity, and unauthorized access. Therefore, it is critical to combat the increased counterfeiting and continuously thwart information from being cloned. In recent years, significant efforts<sup>1–4</sup> have been made to develop both information-storage materials and data-encryption techniques that can ensure the secure storage and transmission of information and achieve advanced information anti-counterfeiting protection. Specifically, anti-counterfeiting technology, such as codes (1D barcodes,<sup>5</sup> 2D black and white code,<sup>6</sup> 3D color code,<sup>7,8</sup> and 4D codes with stimulus-responsiveness<sup>9</sup>), laser holography,<sup>10</sup> watermarks, and luminescent patterns<sup>11</sup> have been explored and applied in production and life to facilitate the identification of authenticity by users. Moreover, information-encryption technology

<sup>a</sup> Key Laboratory of Marine Materials and Related Technologies, Zhejiang Key Laboratory of Marine Materials and Protective Technologies, Ningbo Institute of Materials Technology and Engineering, Chinese Academy of Sciences, Ningbo 315201, China. E-mail: lexiaoxia@nimte.ac.cn, tao.chen@nimte.ac.cn

<sup>b</sup> School of Chemical Sciences, University of Chinese Academy of Sciences, Beijing 100049, China

<sup>c</sup> College of Material Chemistry and Chemical Engineering, Key Laboratory of Organosilicon Chemistry and Material Technology, Ministry of Education, Hangzhou Normal University, Hangzhou 311121, China



(mathematical or physical methods) can combine ordinary information with a secret key to produce a secure ciphertext, so as to further safeguard information during transit and storage.

Stimulus-responsive polymers (SRPs) can show obvious changes, including luminescence,<sup>12–14</sup> discoloration,<sup>15–18</sup> deformation,<sup>19,20</sup> movement,<sup>21</sup> and their combinations,<sup>22</sup> in response to specific external stimulus. In particular, their adjustable optical properties have seen SRPs widely utilized in the field of information storage and anti-counterfeiting, and have aroused great interest. Specifically, when exposed to an external stimulus, such as light,<sup>23,24</sup> temperature,<sup>25,26</sup> ions,<sup>27,28</sup> electricity,<sup>29,30</sup> magnetic,<sup>31,32</sup> mechanical force,<sup>33,34</sup> humidity<sup>35,36</sup> (Fig. 1a), such intelligent systems undergo obvious photophysico-chemical characteristics alteration. Generally, the currently developed SRPs serving as information anti-counterfeiting platforms comprise the following six categories, as illustrated in Fig. 1b.

(i) *Physical color SRPs*. First, SRPs with a certain structural color can be obtained by changing the microstructure of materials to make them interact with light (interference,<sup>37</sup> diffraction,<sup>38–40</sup> scattering,<sup>41,42</sup> etc.). Furthermore, converting the observation of the optical path,<sup>43,44</sup> constructing a certain orientation structure of materials to obtain polarization patterns,<sup>45–47</sup> and utilizing holographic photopolymerization to obtain holographic images<sup>48–53</sup> are also effective means to realize physical color-based changes in SRPs. (ii) *Shape memory SRPs*. Shape-memory polymers are typically composed of both stable chemical and revisable physical networks. The process of shape-memory programming involves shape fixing under external stimuli conditions and shape recovery after withdrawal of the corresponding stimulus. (iii) *Phase-transition SRPs*. In these, the dynamic phase-transition process is usually accompanied by a decrease in the optical transparency of the polymer, which is a ubiquitous phenomenon that has been extensively applied in transient information



Ying Shen

Ying Shen graduated from Fujian Normal University with a bachelor's degree in 2022. Currently, she is a PhD student at the Ningbo Institute of Materials Technology and Engineering (NIMTE), Chinese Academy of Sciences, under the supervision of Professor Tao Chen. Her current research interests include fluorescent hydrogels with structural color and their applications in multi-channel dynamic information-display platforms.



Xiaoxia Le

Xiaoxia Le received her PhD degree in polymer chemistry and physics from the Ningbo Institute of Materials Technology and Engineering (NIMTE), Chinese Academy of Sciences (2019). She then joined Tao Chen's group as a postdoctoral research fellow. Currently, she is an associate professor at NIMTE. Her research focuses on the construction and functionalization of stimuli-responsive hydrogels for applications in soft actuator and fluorescent information anti-counterfeiting fields.



Yue Wu

Yue Wu obtained his B.E. (2017) and PhD (2023) degrees from Dalian University of Technology. Then, he joined Tao Chen's group as a postdoctoral research fellow at the Ningbo Institute of Materials Technology and Engineering (NIMTE), Chinese Academy of Sciences. His main research focuses on structural colors, photonic crystals, and Mie scattering.



Tao Chen

Tao Chen (FRSC) received his PhD from Zhejiang University (China) in 2006. After his postdoctoral training at the University of Warwick (UK), he joined Duke University (USA) as a research scientist. He then moved to Technische Universität Dresden (Germany) as an Alexander von Humboldt research fellow. Since 2012, he has been a full-time professor at the Ningbo Institute of Materials Technology and Engineering (NIMTE), Chinese Academy of Sciences. He has published more than 200 papers in the fields of functional and smart polymers. His research interests include smart hydrogels with applications in soft actuators and gel-based anti-counterfeiting.



storage and encryption. (iv) *Fluorescent SRPs*. SRPs can be endowed with tunable luminescent properties through the introduction of emitting sources, such as organic dyes,<sup>54–56</sup> lanthanide complexes,<sup>57,58</sup> luminescent nanoparticles,<sup>59</sup> conductive polymers (CPs),<sup>60</sup> or quantum dots (QDs).<sup>61–63</sup> (v) *AIEgens-based SRPs*. Luminogens that display an aggregation-induced emission (AIE) effect demonstrate a novel photoluminescence (PL) mechanism beyond the conventional aggregation-caused quenching (ACQ) of molecules and represent one of the most important classes of smart luminescent materials. Consequently, the emission intensity and wavelength of AIEgens-based SRPs are flexibly modulated by aggregation of the morphologies of AIE units. (vi) *Phosphorescent SRPs*. Among the afterglow luminescent materials, polymer-based room-temperature phosphorescence (RTP) materials exhibit relatively excellent practicability, due to having rigid polymer matrices that can suppress the non-radiative decay process, which contributes to phosphorescence emission without the necessity for extreme environmental condition.<sup>64</sup> Additionally, there are plenty of regulating factors (*e.g.*, conformation, packing, and structure of the molecules, intermolecular interactions) of phosphorescent SRPs that can provide new insights for the development of anti-counterfeiting systems.

Up to now, the majority of SRP-based anti-counterfeiting materials generally exhibit a single function, therefore suffering

from the risk of a simple single-channel decryption, resulting in a relatively low-security level and an inability to prevent information from being leaked or mimicked. To overcome these drawbacks, more attention has been focused on developing multi-mode or multi-level technologies for obtaining anti-counterfeiting systems with better security. The systems for static information with multi-mode anti-counterfeiting mainly refer to those that display information by changing the optical modes, which means pre-encrypted information can be revealed under certain optical conditions (*e.g.*, polarized light, natural light, ultraviolet light at different wavelengths). As for dynamic information in a multi-level anti-counterfeiting system, the dynamic information demonstration process that arises from the stimulus-responsive behavior is the key point. Nevertheless, the explorations in relevant research are still at the preliminary stage, and no related review has yet provided an in-depth overview of stimulus-responsive polymer materials for multi-mode and multi-level anti-counterfeiting. Hence, this review provides a tutorial overview that summarizes the research developments in SRP-based anti-counterfeiting materials, including the storage of static and dynamic information, and the design strategies of multi-mode and multi-level security and their prospective application scenarios (Fig. 2). On the basis of the changes in the fundamental optical properties of SRPs, such as adjusting the fluorescence intensity/color or

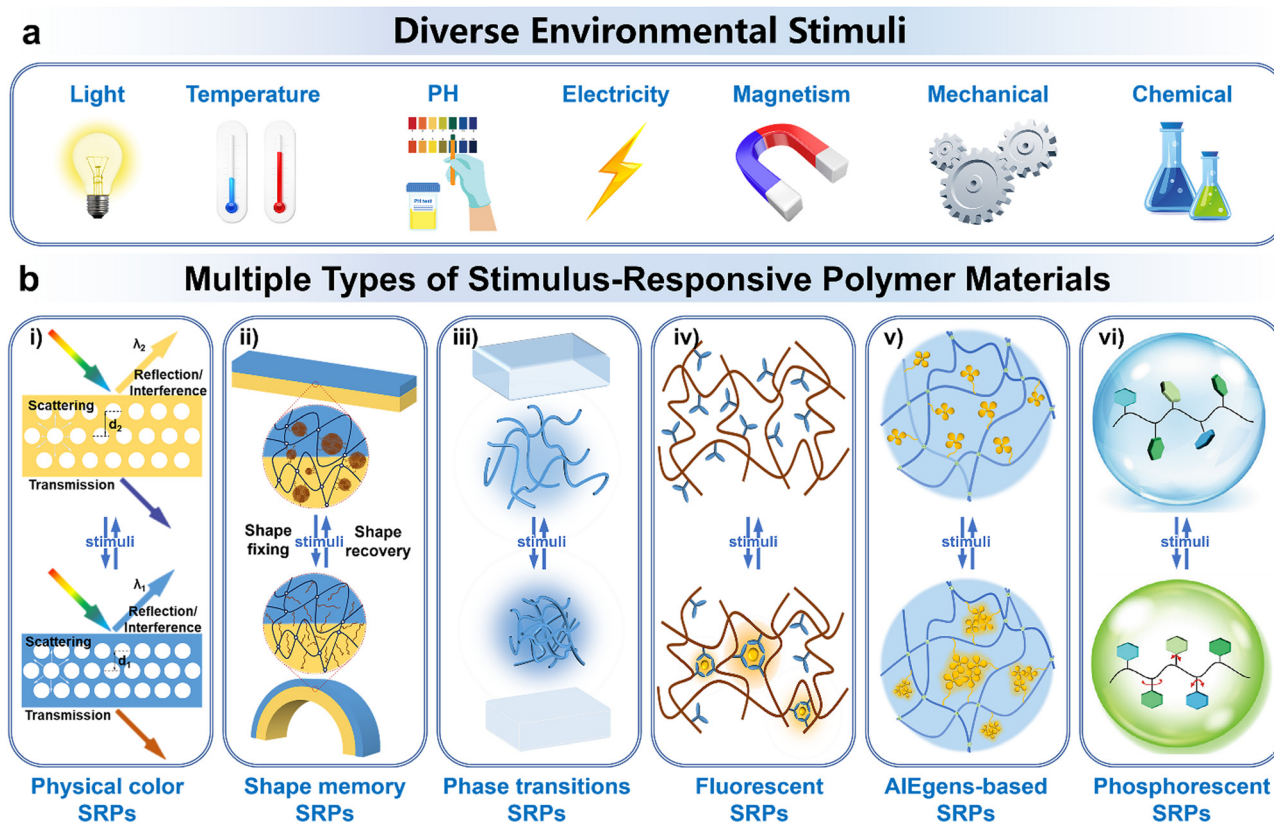


Fig. 1 (a) Common diverse external stimuli, including light, temperature, pH, electricity, magnetism, mechanical force, and chemical solvents. (b) Various stimulus-responsive polymer materials, including (i) physical colored SRPs, (ii) shape-memory SRPs, (iii) phase-transition SRPs, (iv) fluorescent SRPs, (v) AIEgens-based SRPs, and (vi) phosphorescent SRPs.<sup>65</sup> Reprinted with permission from ref. 65 (Copyright 2023 Springer).





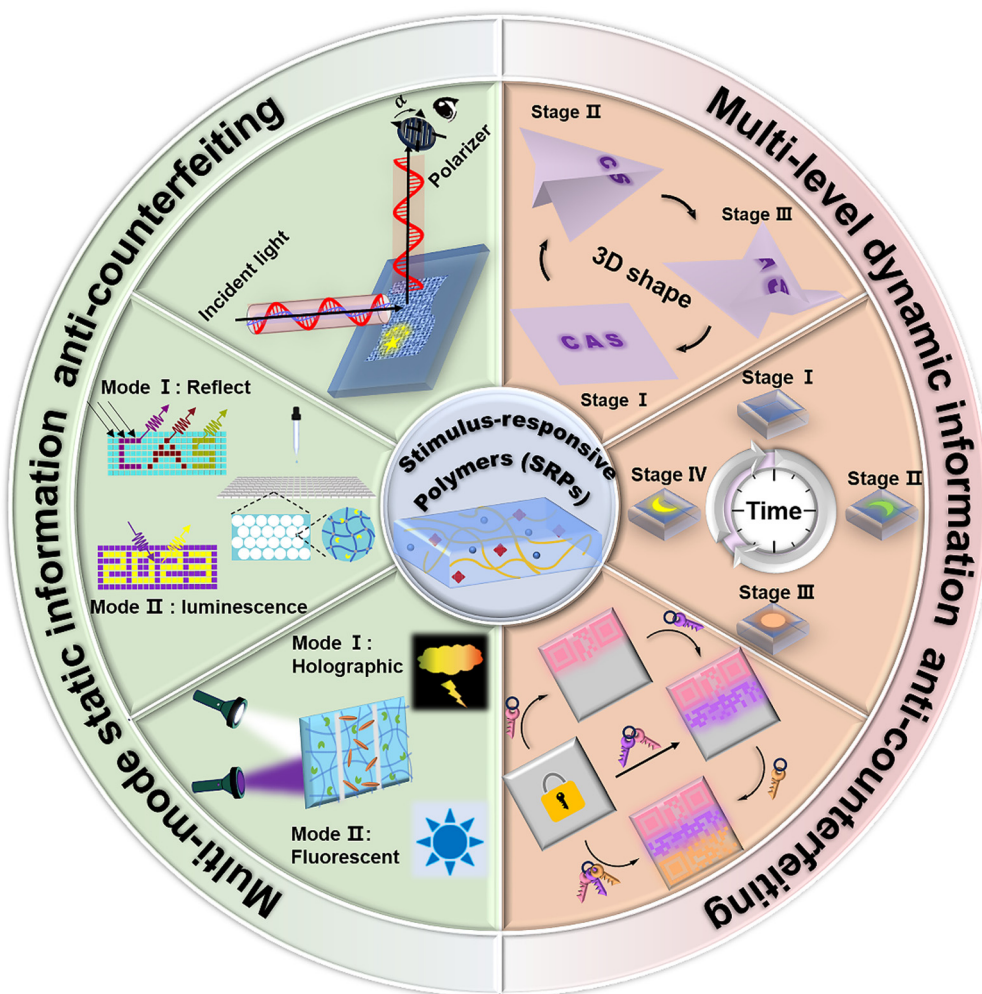


Fig. 2 Overview of the advanced information storage strategies based on stimulus-responsive polymers (SRPs), including multi-mode static information anti-counterfeiting (e.g., the fusion of polarization patterns and fluorescent patterns, the combination of structural color and fluorescence, the integration of holographic information and fluorescence information), and multi-level dynamic information anti-counterfeiting (e.g., extra geometric dimension, added temporal dimension, multiple stimulus responses).

changing the angle of polarized light to display information, multi-mode/multi-level information anti-counterfeiting can be further achieved by combining different optical modes, introducing multi-stimulus response ways, or adding other dimensions (e.g., temporal dimension or/and spatial dimension). Finally, we summarize the current challenges and propose some future perspectives for SRP-based systems toward complex information storage and high-security level anti-counterfeiting technology. We hope that sophisticated anti-counterfeiting systems based on stimulus-responsive polymer materials can foster research toward higher-level information security and more advanced anti-counterfeiting systems.

## 2. Static information with multi-mode anti-counterfeiting

One promising approach that can improve information security is the construction of a multi-mode anti-counterfeiting system,

which shows static multi-mode information under different viewing scenarios. For example, fluorescence, phosphorescence and infrared imaging are the main manifestations of the anti-counterfeiting mode under non-visible light. Besides, the structural colors produced by the photonic crystals, transparency adaptations triggered by the phase transitions, the polarization effects obtained by optical activity materials or chiral structures under polarized light, and other optical phenomena are the primary information-storage modes that function through visible-light channels. In order to obtain a multi-mode anti-counterfeiting system, dual or even multiple optical functional units are usually integrated into one SRP-based anti-counterfeiting material. Currently, various multi-mode anti-counterfeiting systems have been developed, including the combination of structural color and fluorescent color,<sup>66–71</sup> fluorescent patterns working with surface microstructures (wrinkles),<sup>72–76</sup> cooperation of phosphorescence and fluorescence,<sup>77</sup> and excitation-wavelength-dependent luminescence.<sup>78–80</sup> The cutting-edge advancement of multi-mode information encryption/decryption





technologies focuses on designing security anti-counterfeiting materials that can offer numerous optical states to convey the same or distinct information.

## 2.1. Displaying the same information in different optical modes

The storage of multi-modal information in a single system is a promising method for increasing information capacity and improving information security. A common strategy for achieving multi-mode anti-counterfeiting is to integrate fluorescent information under UV light and directly display information under visible light. Zhang's group<sup>66</sup> reported an organohydrogel containing cationic moieties called methacrylamido propyl trimethyl ammonium chloride (MPTAC) and hydrophobic fluorophores of (2-(4-vinylphenyl) ethene-1,1,2-triyl) tribenzene (TPE) in a polyacrylamide gel network (Fig. 3a). Owing to the excellent water absorption, the prepared organohydrogel was able to swell in water, accompanied with a phase-transformation process and the "on-off" switching of fluorescence (Fig. 3b). Aided by laser cutting technology, programmed information (butterfly) can be loaded, which can be encrypted under weak daylight, and then decrypted under both UV light and strong white light during the whole swelling process (Fig. 3c and d). Such water swelling-induced optical switching makes this kind of material stand out in the field of multistage information encryption-decryption.

An increase in the number of optical states is conducive to enhancing the anti-counterfeiting ability to a certain extent.

For example, Wang's team<sup>67</sup> effectively prepared a new large-area and high-quality photonic crystal composite film with three optical states through a molecule-mediated shear-induced assembly technique (MSAT). In this system, the chemical units (lanthanide-doped fluorophore and phosphor with irregular micrometer sizes) were incorporated with a physical colored unit that consisted of PS@PEA core-interlayer-shell (CIS) particles (Fig. 4a and b). With the assistance of a mediating molecule called propylene carbonate, these three kinds of particles could quickly assemble under the action of shear forces, obtaining a composite film with three distinctive optical states. As illustrated in Fig. 4c, a tri-state PC butterfly pattern displayed a structural color, fluorescent emission, and phosphorescence under natural light, UV irradiation (365 nm) and darkness, respectively. This new method of endowing a single pattern with three different display modes significantly improves the security of information.

What's more, Zhang *et al.*<sup>68</sup> demonstrated a convertible humidity-responsive chiral optical film with quadruple optical states for carrying multi-modal information (Fig. 4d and e). Specifically, lanthanide complexes (LCs), cellulose nanocrystals (CNCs), and poly(ethylene glycol) (PEG) were combined *via* a self-assembly method to endow the system with four optical states, including a fluorescent color, chiroptical properties, structural color, and circularly polarized luminescence (CPL). Impressively, without relying on conventional complicated structured encryption techniques, each optical state could be independently coded or incorporated to boost the anti-counterfeiting level.

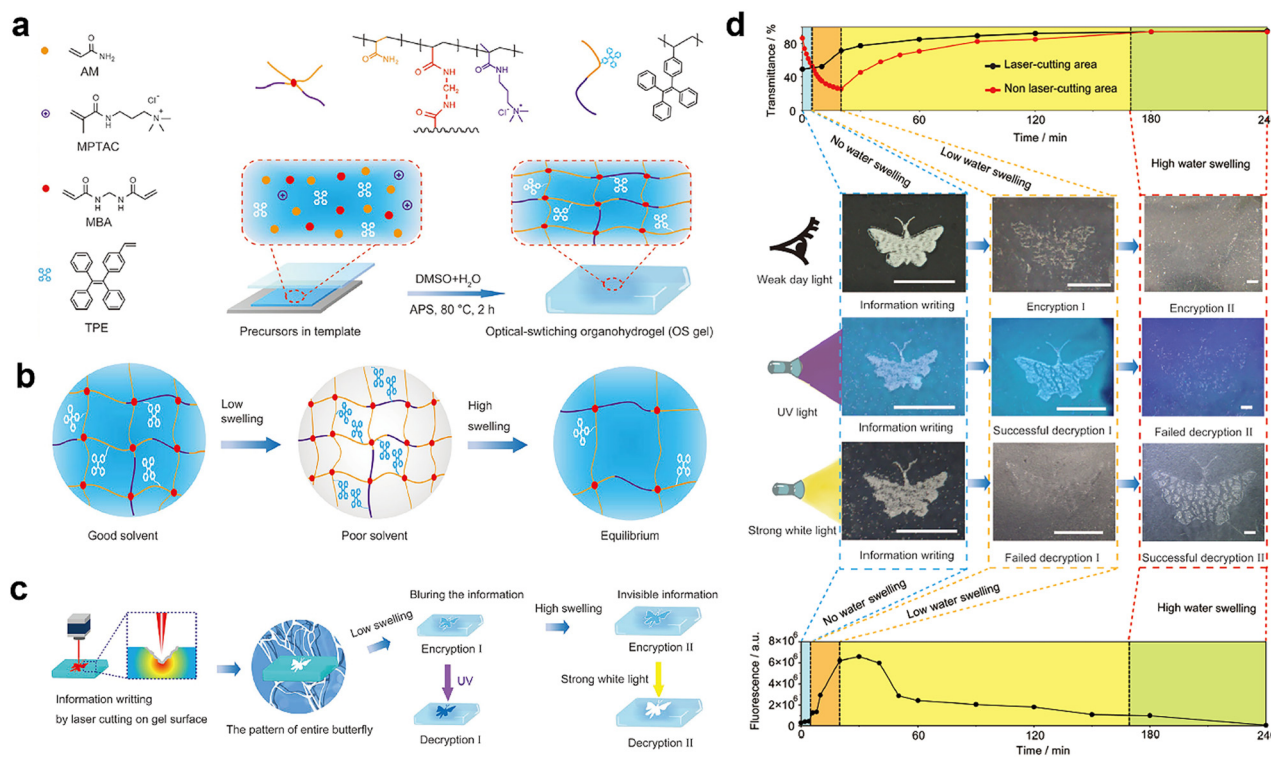


Fig. 3 (a) Design and fabrication of an optical-switching organohydrogel (OS gel). (b) Swelling properties of the OS gel in different conditions. (c) Information encoding and its encryption-decryption process carried out on the surface of the OS gel. (d) Multistage information encryption and decryption based on swelling performance.<sup>66</sup> Reprinted with permission from ref. 66 (Copyright 2022 John Wiley and Sons).



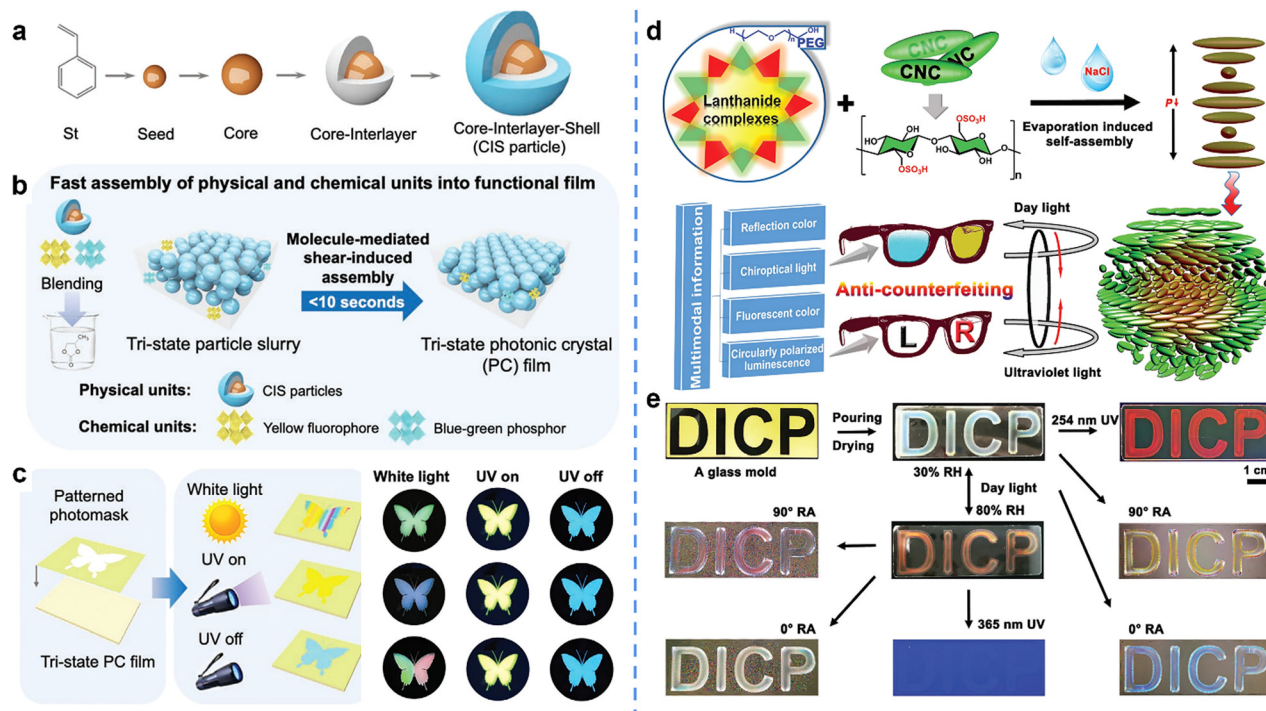


Fig. 4 (a) The preparation process of PS@PEA CIS particles. (b) Schematic of the fabrication of a tri-state photonic crystal composite film. (c) Preparation of patterns on the tri-state PC film and pictures of the obtained patterns under different light conditions.<sup>67</sup> (d) CNC-derived chiral optical films with quadruple optical switching. (e) Multimodal optical conversion of the designed letters "DICP".<sup>68</sup> Reprinted with permission from ref. 67 (Copyright 2023 John Wiley and Sons), and ref. 68 (Copyright 2022 John Wiley and Sons).

It has been well established that excitation-wavelength-dependent (Ex-De) emission materials show excellent potential in multi-mode information storage and anti-counterfeiting fields. Li *et al.*<sup>78</sup> created an integrated system with full-color tunability based on a range of Ex-De room-temperature phosphorescent (RTP) materials by altering the molecular structure. The amorphous RTP systems were effectively produced by an environmentally friendly dehydration condensation process based on aryl boronic acids (e.g., m-Bp-BOH, Nap-BOH, Py-BOH) and polyvinyl alcohol (PVA), as shown in Fig. 5a. When the excitation wavelength was increased from 254 to 312 to 365 nm, the afterglow color of BNP-BOH-PVA was shifted from blue to yellow-green to red. Taking advantage of silk screen printing, multi-level information encryption (two QR codes) could be realized by using m-Bp-BOH-PVA and Py-BOH-PVA as inks (Fig. 5b). In contrast to conventional multicolored patterned luminescent materials, the present system possessed the advantage of high discriminability upon UV excitation at different wavelengths and an easy preparation process.

Similarly, Zhao's group<sup>80</sup> reported a series of excitation-dependent long-life luminescent polymers (ED-LFLPs) that extended the emission color range from blue to red, which were used to construct anti-counterfeiting patterns with multi-colored interconversion under different ambient conditions. These ED-LFLP systems were fabricated by doping simple pyrene derivatives (Fig. 5c), namely 1-pyrenemethanol (PYM), 1-hydroxypyrene (HPY), 1-pyrenecarboxylic acid (PCA), and 1-pyrenylboronic acid (PBA), into the robust polyvinyl alcohol

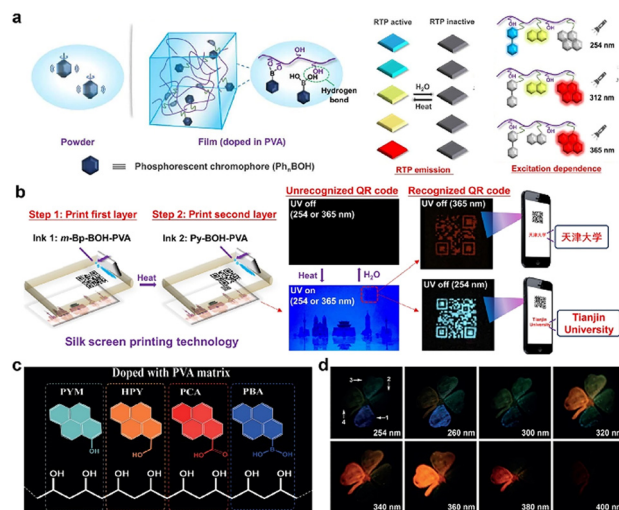


Fig. 5 (a) Room temperature phosphorescent system (BNP-BOH-PVA film) with stimulus-responsive color variation. (b) BNP-BOH-PVA films for information encryption with the assistance of silk screen printing.<sup>78</sup> (c) The composition of ED-LFLP systems. (d) Multicolor four-leaf clover anti-counterfeiting pattern with multi-mode phosphorescence.<sup>80</sup> Reprinted with permission from ref. 78 (Copyright 2022 American Association for the Advancement of Science), and ref. 80 (Copyright 2020 John Wiley and Sons).

(PVA) matrix. A four-leaf clover pattern was designed on paper by exploiting doped polymer inks, where the numbers 1–4 of petals referred to PBA-PVA, HPY-PVA, PYM-PVA, and PCA-PVA,



respectively (Fig. 5d). Briefly, the multicomponent clover pattern's afterglow displayed a range of colors when exposed to diverse wavelengths of UV light, and the intent was to apply this in multi-mode anti-counterfeiting. However, it is a pity that this kind of pattern requires multiple components to piece together independently, while the shifts in color seemed analogous and hard to differentiate at various wavelengths.

## 2.2. Display of different information in distinct optical modes

Compared with displaying the same information in different optical modes, it is more challenging to independently show different information in distinct optical channels. The main reason for this is that it is difficult to avoid mutual interference between different information elements during the preparation and later usage of the materials. To address the above challenges, Qin *et al.*<sup>69</sup> developed a series of fluorescent cholesteric liquid crystal (FCLC) microdroplets, exhibiting rich reflection colors under the illumination of white light and fluorescent color under the excitation of UV light. The structural color was controlled by the photonic crystals “coated”-helical superstructure in CLC, which could be adjusted by changing the content of the chiral dopant, while bright cyan fluorescence was determined by the molecular structure of the FCLC microdroplets. As a result, a geminate label carrying the RGB letters “FDU” and fluorescent pattern “I♥U” were encoded in an array by integrating different FCLC microdroplets (Fig. 6). This anti-counterfeiting label possessed both a reflective state and fluorescent state, which could demonstrate two distinct kinds of information, which was expected to improve anti-counterfeiting efforts and promote the evolution of anti-counterfeiting technology.

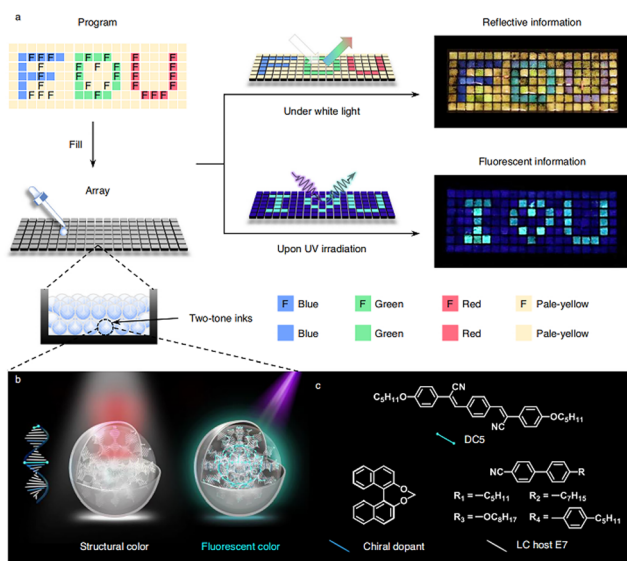


**Fig. 6** Geminate labels carrying two distinct kinds of information under white and UV light, respectively. (a) Schematic illustration of a geminate label with two different information items of an “FDU” reflective pattern and an “I♥U” fluorescent pattern. (b) Chemical structures of the materials used to prepare the FCLC mixtures, which show structural color under white light and fluorescent color under UV light.<sup>69</sup> Reprinted with permission from ref. 69 (Copyright 2021 Springer).

Holographic patterns and fluorescent patterns that can be respectively displayed under natural light and ultraviolet light are also an effective combination for achieving dual-mode anti-counterfeiting. Zhao *et al.*<sup>71</sup> designed a method involving the crosstalk-free patterning of holographic and fluorescent images by the synergy of an AIEgen (aggregation-induced emission luminogen) with a liquid crystal (LC) (Fig. 7a). Specifically, a holographic image could be created by a photopolymerization-induced phase separation and the fluorescent image could be patterned through the photocyclization of AIEgen (Fig. 7b). In addition, the novel AIEgen/LC system showed fluorescence variation and phase transition under external thermal stimulation, resulting in synergistic changes of the dual-mode information (Fig. 7c). Notably, this research not only resolved the conventional interference issue to obtain crosstalk-free images within a double optical mode but also a cooperative-thermo-response property to realize information manipulation in various modes in reaction to external stimuli.

Another typical example was presented by Xu *et al.*<sup>81</sup> who constructed a noninterfering chromatic polarization pattern and photonic pattern on a photoresponsive azopolymer P1 *via* a unique orthogonal photopatterning approach (Fig. 8a and b). As the azopolymer exhibited photoinduced reversible solid-to-liquid transitions, the photonic patterns on the P1 film could be adjusted by masked nanoimprinting (Fig. 8c). What's more, P1 also displayed excellent stretchability, and chromatic polarization patterns could be obtained by stretching and the irradiation of polarized light with a photomask (Fig. 8d). The above dual-mode patterns were noninterfering and could be written repeatedly by utilizing photo-, thermal-, or solution reprocessing, which paves the way for creating photo-patternable materials and multi-mode patterning methods.

In addition, multi-mode anti-counterfeiting can also be achieved by simply changing the spatial distribution of light, such as the amplitude, phase, and polarization. For instance, Lai *et al.*<sup>82</sup> developed a new strategy to fabricate a polarization-sensitive photonic crystal composite film (PCCF) with a quasi-3D photonic architecture *via* a simple self-assembling and nanoimprinting technique (Fig. 9a). The created composite lattice photonic crystal architecture exhibited multiple optical effects, such as scattering, polarization, and diffraction, endowing PCCF with the properties of full pixel multiplexing, multi-channel cryptography, and the full spatial control of light. As depicted in Fig. 9b, a QR code cryptographed with PCCF could only be scanned when viewed from the other side of the incident light and the polarizer was rotated to 90°. Therefore, this strategy that gives material multichannel images can dramatically increase the storage capacity, as well as improve the security of information.

## 3. Dynamic information with multi-level anti-counterfeiting

For dynamic information with multi-level anti-counterfeiting, extra parameters (*e.g.*, chromaticity, geometry, time, space) are





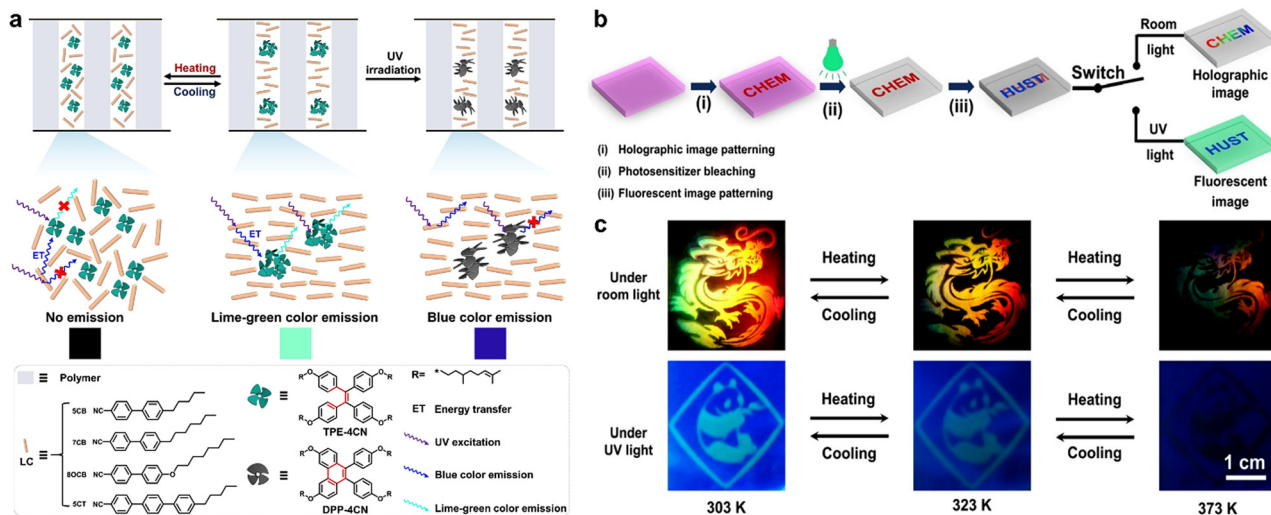


Fig. 7 Liquid crystal (LC)/AIEgen system for patterning crosstalk-free images. (a) Synergistic mechanism for obtaining a holographic pattern and fluorescent pattern in the LC/AIEgen system. (b) Coding procedure for the holographic and fluorescent images. (c) Cooperative-thermoreponse behaviors of the holographic and fluorescent images under room light and UV light, respectively.<sup>71</sup> Reprinted with permission from ref. 71 (Copyright 2020 John Wiley and Sons).

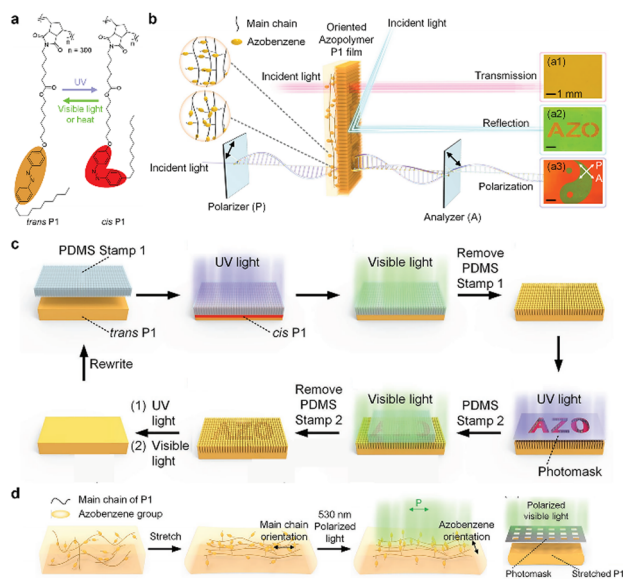


Fig. 8 Rewritable dual-mode patterns based on a photoresponsive azopolymer P1. (a) Diagram of *cis-trans* photoisomerization of P1. (b) Schematic and images of an azopolymer P1-patterned film that was captured in the (a1) transmission, (a2) reflection, and (a3) polarization modes. (c) Process of patterning photonic structures on the P1 film. (d) Process of preparing chromatic polarization patterns on P1 film.<sup>81</sup> Reprinted with permission from ref. 81 (Copyright 2022 John Wiley and Sons).

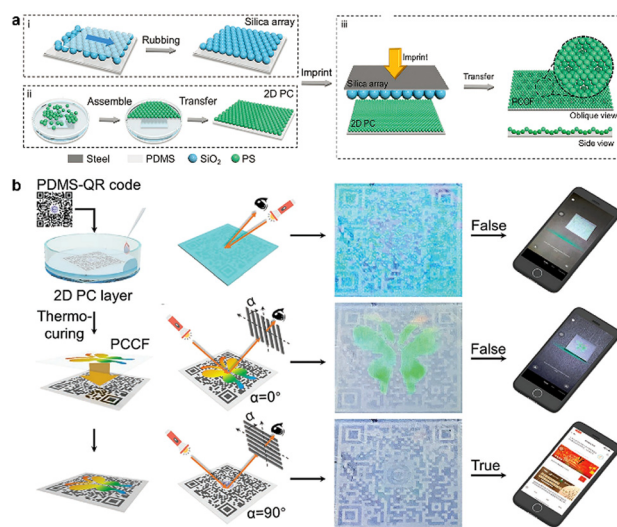


Fig. 9 Quasi-3D multiplexed anti-counterfeiting imaging. (a) Process flow diagram for the manufacture of (i) the 2D PC, (ii) the MSCT, and (iii) the PCCF. (b) Encoding and decoding of the PCCF-encoded paper-printed QR code under different viewing modes.<sup>82</sup> Reprinted with permission from ref. 82 (Copyright 2022 John Wiley and Sons).

usually introduced to increase the difficulty of decryption in comparison to multi-mode static patterns. The involved dynamic process refers to triggering the emergence of hidden information in SRPs in response to either a single external stimulus or a combination of several stimuli. According to the differences in the decrypted information, currently developed multi-level anti-counterfeiting strategies based on SRPs can be divided into the

following two types: the progressive display of target information and step-by-step presentation of different information. The former aims to get the final target information by undertaking a series of decryption steps, including color fluctuation, shape morphing, self-healing, and other processes. The latter aims to display multiple pieces of information in a decryption process, and these pieces of information can either be true/false or have certain relationships. Alongside this, researchers have also reported plenty of paradigms to tune the emission intensity and color diversity or used multiple stimuli as collaborative keys<sup>83–89</sup>

for encoding intricate information. These works are inspiring and motivating and have made it possible to code and decrypt multi-level information.

### 3.1. Progressive display of target information

A crucial point for the progressive display of target information is to organize and combine varied responsiveness in one stimulus-responsive polymer system, which remains a substantial difficulty due to the diverse response mechanisms and their compatibility. To address this disadvantage, the exploration of different manifestations either under the same stimulus or several stimuli so as to obtain the hidden target information is in severe demand.

The assembly of materials with different stimuli-responsiveness could attain encrypted information with a higher decoding security. Zhang *et al.*<sup>83</sup> successfully prepared three different stimulus-responsive polymers, containing the same poly(methyl methacrylate) (PMMA) main chains, 2-ureido-4-pyrimidone (UPy) recognition units, and three different chromogenic subunits. These polymers could self-assemble through hydrogen-bonding interactions to form supramolecular gels (G1, G2, G3), which produced pink, purple, and yellow colors in response to acetic acid vapor, UV light, or methanolic FeCl<sub>3</sub>, respectively. As shown in Fig. 10a, G5 with a QR pattern can be obtained by assembling G1, G2, and G3 by interfacial adhesion and a further engraving. Only when the above-mentioned stimuli were all applied simultaneously could the full stored information be revealed (Fig. 10b).

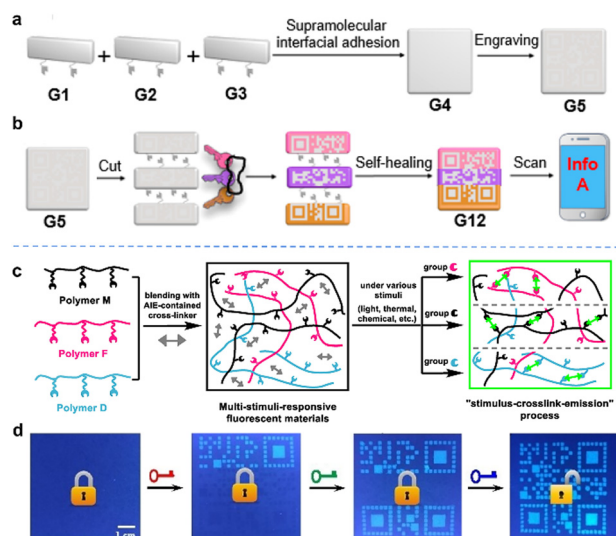


**Fig. 10** Multi-stimuli-responsive fluorescent materials for information encryption/decryption. (a) Formation of G5 that was engraved with a QR pattern. (b) Illustration showing the QR pattern on G5 could be easily scanned when three different stimuli (pink key represents HOAc vapor, purple key represents UV light, and yellow key represents FeCl<sub>3</sub>/CH<sub>3</sub>OH) were applied.<sup>83</sup> (c) Multi-stimuli-responsive materials were prepared by blending different linear polymers and the AIE-contained cross-linker. (d) Images showing the stored QR pattern on the multiple-encryption system could only be observed when all three different stimuli were applied.<sup>87</sup> Reprinted with permission from ref. 83 (Copyright 2021 American Chemical Society), and ref. 87 (Copyright 2022 John Wiley and Sons).

This ingenious information encryption strategy attained a higher level of decoding security. Nevertheless, it is a pity that it still has significant application scenario limitations such that when the background color was changed to black or other colors with sharp contrast to the pattern, the QR code could be directly read without elaborate stimulation keys.

The above problems can be skillfully avoided by utilizing multi-stimuli-responsive fluorescent materials. For example, Jiang and colleagues<sup>87</sup> developed a series of polymer solution inks, which consisted of linear polymers with various stimulus-sensitive moieties and an AIE cross-linker. As shown in Fig. 10c, the linear polymer could crosslink with the cross-linker to create networks in response to stimuli, which inherently limited the AIE molecule's ability to rotate intramolecularly and produce intense emissions. A three-part QR pattern, each printed with a different ink, could show the stored information "SCUEC" after being treated with all three stimuli and under UV light through the planned "stimulus-crosslink-emission" pathway (Fig. 10d). This tactic guarantees the adaptability of behavioral stimulus-response logic and a compatibility of various stimuli-responses, and these fluorescent materials with multiple stimulus responses have shown excellent accessibility and adaptability for data encryption.

Compared to planar surfaces, encryption on 3D objects adds an extra geometric dimension and thus possesses a much higher level of security. As presented in Fig. 11, a nonplanar information coding tactic was established by Chen *et al.*<sup>90</sup> that allowed the independent control of visible light for the 3D printing of a hydrogel and ultraviolet light for encoding fluorescent information. It was possible to generate hydrogels in a variety of complicated geometries, and subsequent UV patterning enabled the surface to be activated in a spatioselective manner for encoding fluorescent information through the orthogonal photochemistry method (Fig. 11a). For instance, the information (the "maze" image) could only be correctly retrieved if the parts were put together in a specific way to simultaneously match the shape and luminous pattern (Fig. 11b). In addition, a more sophisticated pumpkin-lantern-shaped hydrogel obtained by 3D printing was encoded with different messages on different sides. The whole information "ARE YOU HERE" could be observed when reading clockwise under UV light (Fig. 11c). Obviously, making macroscopic geometry and surface fluorescence images work together can create high-security encryption that goes beyond conventional 2D encryption.

In another typical example, we developed a 3D anti-counterfeiting platform based on perylene-tetracarboxylic-acid-functionalized gelatin/poly(vinyl alcohol) hydrogels for multistage data security protection.<sup>91</sup> The as-prepared hydrogel displayed an Fe<sup>3+</sup>-triggered fluorescence quenching performance, indicating that Fe<sup>3+</sup> can be used as ink for information loading. Besides, borax-induced shape memory and self-healing behaviors endowed the hydrogels with programmable 3D geometries, leading to multistage information storage by further incorporating 3D origami techniques (Fig. 12). As a result, the unique anti-counterfeiting platform exhibited a higher level of security than the traditional 2D counterparts.





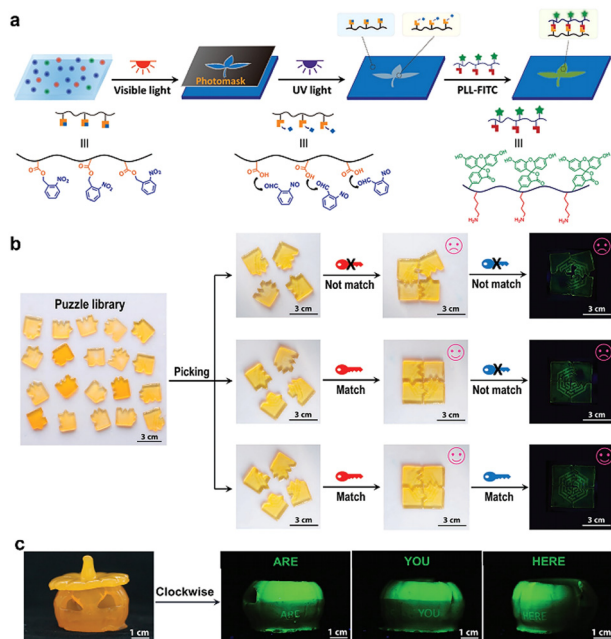


Fig. 11 3D-printed hydrogel for information encryption. (a) Mechanism of hydrogel curing and patterning via orthogonal photochemistry. (b) Multi-stage encryption based on a puzzle library. (c) Various words were encoded on different sides of a hydrogel pumpkin lantern.<sup>90</sup> Reprinted with permission from ref. 90 (Copyright 2023 John Wiley and Sons).

### 3.2. Step-by-step presentation of different information

The gradual display of different information means that multiple pieces of information will emerge during the entire information decryption process, and these pieces of information may need to be authenticated or mutually corroborated to get the final information. Generally, there are two different ways to progressively present different information: (i) multi-stimulus response systems can be constructed to realize gradual deciphering by programmed external stimuli; (ii) a time dimension can be introduced to present different information at different times under a single stimulus. Following these two lines, numerous step-by-step presentations of different information for multi-level information encryption/decryption have been reported.

Lan *et al.*<sup>92</sup> reported a novel strategy to fabricate fluorescent hydrogels with multi-level information encryption/decryption functionalities by adjusting homocrystalline (HC) and stereo-complex (SC) crystal phases. As shown in Fig. 13a, a poly(acrylic acid)-*g*-PLLA (PAA-*g*-PLLA) hydrogel was first prepared as a substrate, in which tetraphenylethene (TPE)-modified PLLA (TPE-PLLA), and PDLA (TPE-PDLA) could permeate into when dissolved in acetone solution. By using solvent-assisted diffusion and solvent exchange, TPE-PLLA and TPE-PDLA could produce the HC and SC crystal phases to encode completely different information, respectively. In view of the different solvent resistances, the HC and SC crystal phases endowed the hydrogel with differential variations in transparency and fluorescence. When soaked in DMSO, a highly programmable QR code was concealed under visible light. Once exposed to UV

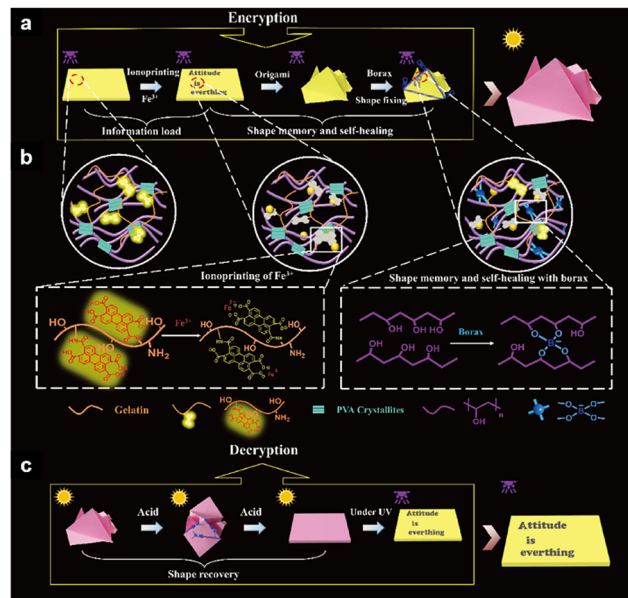


Fig. 12 3D fluorescent hydrogel for multistage data security protection. (a) and (b) The encryption process, which contains information loading, shape memory, and a self-healing procedure. (c) The decryption process, including sequential shape recovery and UV irradiation.<sup>91</sup> Reprinted with permission from ref. 91 (Copyright 2019 John Wiley and Sons).

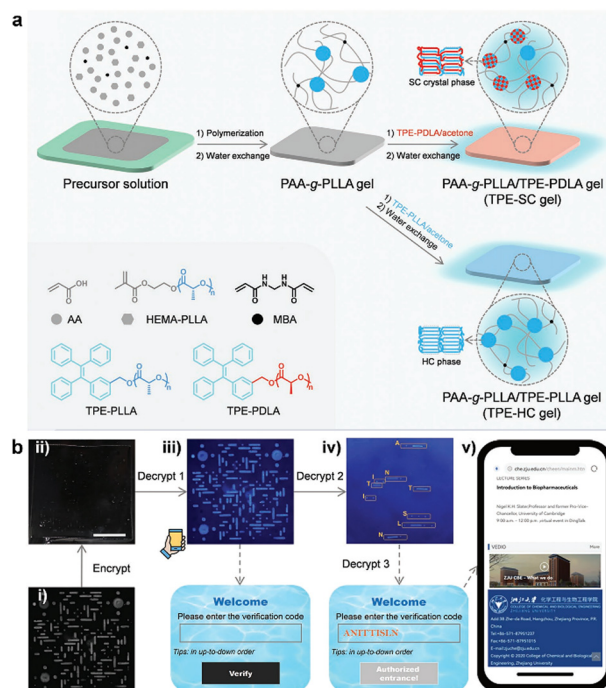


Fig. 13 Multi-level information encryption/decryption based on programmable crystal phases in fluorescent hydrogels. (a) Designs of PAA-*g*-PLLA gel, TPE-SC gel and TPE-HC gel. (b) Image showing the complicated QR code with HC and SC crystal phases, exhibiting multi-level encryption/decryption under UV irradiation and solvent replacement.<sup>92</sup> Reprinted with permission from ref. 92 (Copyright 2023 John Wiley and Sons).

light, the QR code appeared and could be scanned to obtain a login window. Further, the corresponding verification code



could be obtained by replacing the solvent with acetone, achieving a complete decryption (Fig. 13b). This research puts forward the idea that crystal phase programming can serve as a potent paradigm for creating hydrogel materials that are more secure against counterfeiting.

Through the combination of ultraviolet light and mechanical stretching, Tang's group<sup>93</sup> pioneered a fluorescent nanocomposite (NC) hydrogel with the ability to promote information-storage expansion. They designed a pH-responsive AIEgen named (Me<sub>2</sub>N)<sub>2</sub>-TPE-Py, which could be protonated under acidic conditions and bonded with a negatively charged nanoclay (LAPONITE<sup>®</sup> XLS) by electrostatic interaction (Fig. 14a). Then, the target hydrogel could be obtained by embedding the AIEgens in a poly(acrylamide) (PAAm)/LAPONITE<sup>®</sup> XLS-based NC hydrogel, which exhibited a remarkable enhancement of the blue-shifted emission under the stimulus of the acid. With the assistance of suitable molds with H<sup>+</sup> solution, various information could be encoded into the hydrogel both in the original and stretched states (Fig. 14b). Consequently, hierarchically stored information, including a QR code and two barcodes, could be sequentially displayed under UV irradiation and mechanical stretching (Fig. 14c). This strategy could not only realize multi-level information storage but could also greatly expand the storage capacity of information.

Recently, we also achieved multi-level information storage by constructing a urease-containing fluorescent hydrogel.<sup>55</sup> The fluorescent hydrogel-based information platform was synthesized by copolymerizing the protonated fluorescent monomer 4-(*N,N*-dimethylamino ethylene) amino-*N*-allyl-1,8 naphthalimide (DEAN-H<sup>+</sup>) with acrylamide. Since the decomposition of urea was catalyzed to produce NH<sub>3</sub> in the presence of urease, the naphthalimide moieties of DEAN could thus be deprotonated which caused fluorescence quenching. Moreover, various metal ions (e.g., Zn<sup>2+</sup>, Al<sup>3+</sup>) could coordinate with DEAN and be eliminated sequentially upon NH<sub>3</sub> condition, leading to the fluorescence programmable on-off performance. Therefore,

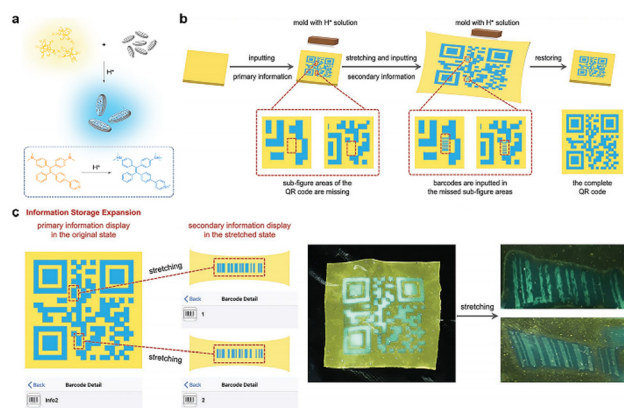


Fig. 14 (a) Interactions between (Me<sub>2</sub>N)<sub>2</sub>-TPE-Py and LAPONITE<sup>®</sup> XLS under acid stimulation. (b) The encoding process of multiple information, including a QR code and two barcodes. (c) The decryption of hidden QR code and barcodes under UV irradiation and mechanical stretching.<sup>93</sup> Reprinted with permission from ref. 93 (Copyright 2022 John Wiley and Sons).

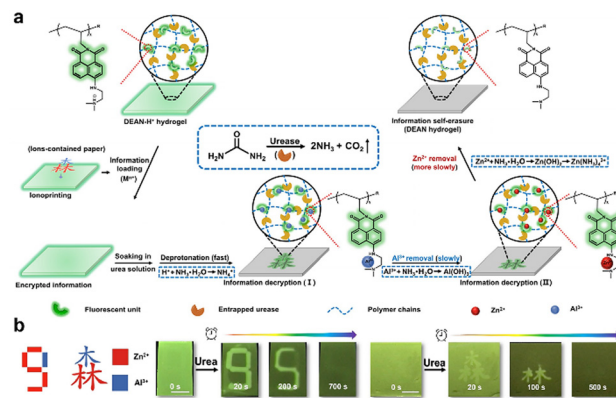


Fig. 15 (a) Schematic illustration of urease-containing fluorescent hydrogel for instantaneous multi-level fluorescence information storage. (b) Encryption-decryption-self-erasing process of encoded information during the urease-urea catalyzed reaction.<sup>55</sup> Reprinted with permission from ref. 55 (Copyright 2021 John Wiley and Sons).

the concealed information created by the metal ions could be presented sequentially in urea solution before finally dissipating, giving the fluorescent hydrogel the ability to decrypt information according to the time dimension (Fig. 15a). For instance, the hidden information “9” and “forest” emerged at first, but then turned to “5” and “forest”, respectively, during the decryption process (Fig. 15b). Finally, all the information vanished, thus achieving multi-level information storage with a self-erasing performance. In a nutshell, such information encryption materials with a time-dependent characteristic are of great significance to the improvement of information security.

In another example, we developed a photochromic fluorescent organohydrogel for dynamic anti-counterfeiting.<sup>56</sup> The organohydrogel was composed of a poly(*N,N* dimethylacrylamide) (PDMA) hydrogel network with green-yellow naphthalimide units (DEAN) and a polyoctadecyl methacrylate (PSMA) organogel network with photochromic spiropyran moieties (SP) via a two-step interpenetrating technique (Fig. 16a). The original

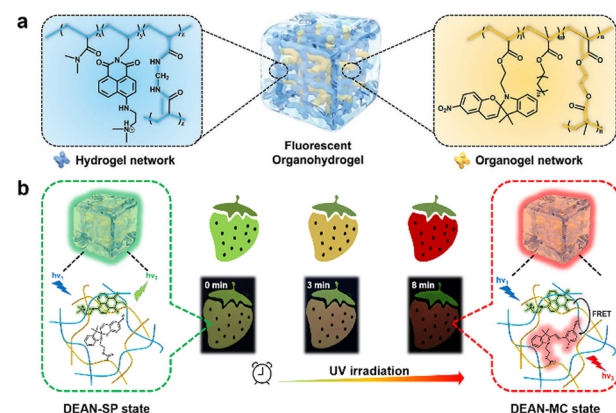


Fig. 16 (a) Schematic illustration of a fluorescent organohydrogel made up of a hydrogel network and organogel network. (b) Photos and mechanism of fluorescence discoloration during the process of ultraviolet illumination.<sup>56</sup> Reprinted with permission from ref. 56 (Copyright 2021 John Wiley and Sons).



organohydrogel emitted yellow-green fluorescence, which could be converted to red fluorescence due to the fluorescence resonance energy-transfer (FRET) process that occurred between DEAN and the opened merocyanine units (MC). As shown in Fig. 16b, the strawberry-shaped organohydrogel underwent a fluorescent discoloration that changed from green to orange and finally red with the extension of the UV irradiation time. In this work, the time dimension was introduced for realizing dynamic color changes and enhancing information security.

Moreover, Xie *et al.*<sup>94</sup> utilized the tactic of coordinating with various metal ions to demonstrate time-gated discoloration four-dimensional (4D) soft patterns generated from an AIE-active polymeric gel (PTPEG). As shown in Fig. 17a, the core of the PTPEG was a tetraphenylethene (TPE)-based salicylaldehyde benzoylhydrazone multi-armed AIEgen (TPE-4SAH), which was prepared by TPE-cored-salicylaldehyde (TPE-4SA) and linear acylhydrazine-terminated PEG (PEG-2AH). The metal-coordinated TPE-4SAH system showed a UV-mediated fluorescence change behavior attributed to a mechanism involving photo-triggered aggregation-induced emission (PTAIE) and excited-state intra/intermolecular proton-transfer (ESPT) processes. Moreover, the binding ability of different metal ions ( $\text{Al}^{3+}$ ,  $\text{Zn}^{2+}$ , and  $\text{Cd}^{2+}$ ) supported the PTPEG/metal-ion systems' varying emission wavelengths and fluorescence response rates in the presence of UV irradiation. The encrypted 3D pattern employing varied ion layers on nine identical flaky PTPEG gels, respectively, and through a self-heal ability exhibited a discoloration decryption behavior with UV irradiation time dependency (Fig. 17b). Overall, multi-level security displays also can be implemented with dynamic 4D patterns.

In addition to time-dependent fluorescent SRPs, organic ultralong RTP materials with temporal-specific emission have promising applications in multi-level anti-counterfeiting. According to Wang *et al.*,<sup>95</sup> a time-dependent organic long

persistent luminescence system was successfully constructed with the assistance of an efficient phosphorescence resonance energy-transfer (PRET) process between the energy donor and acceptor (Fig. 18a). As shown in Fig. 18b, the original word "NEVER" (where the word 'NEVER' was composed of 15% RhB@PVA ('N'), 5% Rh6G/5,7-ICz@PVA ('EVE'), and 15% Fluo/11,12-ICz@PVA ('R'), respectively) with multicolor fluorescence could be turned successively into "EVER" and "EVE" after removing the UV irradiation at different duration times. Notably, carrying distinguishable lifetime codes offers new opportunities for effective anti-counterfeiting platforms with high-security levels.

Another preparation strategy for RTP materials with time-resolved emission characteristics is to regulate the strength of the hydrogen-bonding interactions. In this vein, Xiong *et al.*<sup>96</sup> synthesized pyridine-substituted triphenylamine derivatives doped PVA and PMMA systems (Fig. 18c), which integrated an ultralong lifespan, multicolor afterglow, and reversible reaction to UV irradiation, providing a reference for applications in multi-level anti-counterfeiting. As depicted in Fig. 18d, TPA-2Py@PMMA, TPA-2Py@PVA, 20% RhB/TPA-2Py@PVA, and 10% RhB/TPA-2Py@PVA made up the encryption pattern, respectively. The numbers "8", "9", and "7" were successfully gradually presented after removing the transient UV irradiation; meanwhile, when continuous UV irradiation was applied to the multicolor fluorescence number "8", the afterglow numbers "8" and "7" with different duration times appeared successively. Generally, the way to construct multi-level information encryption platforms based on RTP materials seems to offer more possibilities for developments in this field.

Inspired by the states of bread baking under different temperatures and times, Lou *et al.*<sup>97</sup> presented a novel approach for "double-lock" information camouflage and multi-level encryption under both time and temperature dimensions by employing thermosensitive polymer hydrogels with a lower critical solution temperature (LCST) and upper critical solution temperature (UCST) (Fig. 19a). By precisely regulating the critical point temperature ( $T_{\text{cp}}$ ) and phase-transition time, the double-lock label consisting of poly(*N*-isopropylacrylamide-*acrylamide*) hydrogel (L-AM<sub>x</sub>-BIS<sub>y</sub>) and poly(*N,N*-dimethyl(acrylamidopropyl)) ammonium butane-sulfonate acrylamide hydrogel (U-AM<sub>x</sub>-BIS<sub>y</sub>) could be possibly exploited to encode and decode complicated information on scales based on both time and temperature. As demonstrated in Fig. 19b, the double-lock encrypted QR code could only be recognized in a certain time period at a specific temperature. Clearly, double-lock encryption technology that combines time and temperature dimensions is a powerful means for improving information security.

Similarly, Song's group<sup>98</sup> reported a novel photonic anti-counterfeiting ink with synergistic time- and temperature-solved encryption/decryption properties. The structural colors of photonic inks made up of hydroxypropyl cellulose (HPC)/propylene glycol (PG) mesophases could be regulated by their own composition and external temperature, achieving a transition from completely colorless and transparent to the entire visible-light region (Fig. 19c). Based on the above, multiple

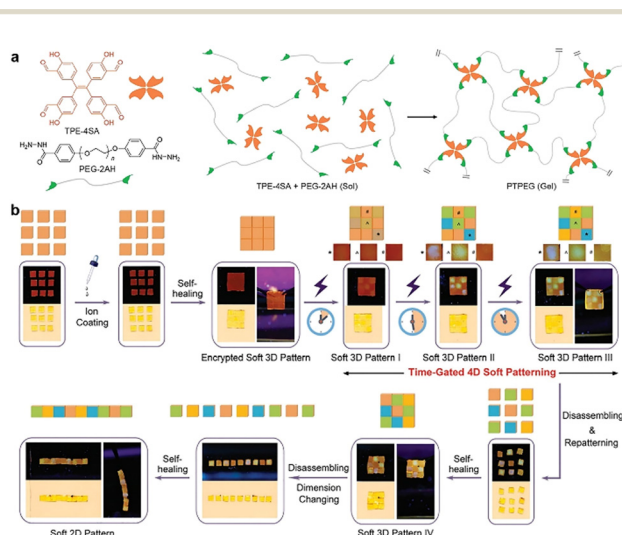


Fig. 17 (a) Diagrammatic representation of the PTPEG gel preparation process. (b) The photos of time-gated 4D soft pattern generated from PTPEG gel coating with ions.<sup>94</sup> Reprinted with permission from ref. 94 (Copyright 2021 John Wiley and Sons).





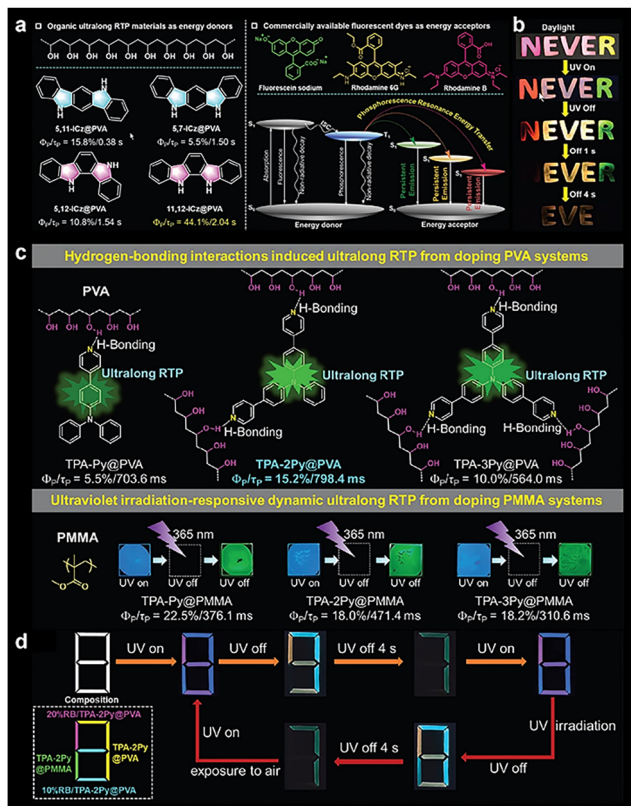


Fig. 18 RTP material with time-resolved emission characteristics for multi-level anti-counterfeiting. (a) The chemical structures of 5,11-ICz@PVA, 5,7-ICz@PVA, 5,12-ICz@PVA, and 11,12-ICz@PVA, and commercially available fluorescent dyes. (b) A demonstration of multi-level anti-counterfeiting application.<sup>95</sup> (c) The chemical structures of the guest phosphors TPA-Py, TPA-2Py, and TPA-3Py, as well as their RTP characteristics upon doping in the PVA and PMMA, respectively. (d) The composition and photos of multi-level anti-counterfeiting and information encryption patterns.<sup>96</sup> Reprinted with permission from ref. 95 (Copyright 2023 John Wiley and Sons), and ref. 96 (Copyright 2023 John Wiley and Sons).

messages, including “ABCD”, “ACBD”, and “ADBC”, stored in different channels could be independently displayed at their appointed temperature point (Fig. 19d). Additionally, “true” information corresponding to Morse code could be sorted out from the “false” information by controlling the time points (Fig. 19e). The above reveal that information-storage security and decoding complexity can be increased by using multi-level encryption techniques like multichannel coding in a stacking mode. Meanwhile, this work makes the design and development of dynamic photonic inks and sophisticated encryption techniques for high-end anti-counterfeiting applications possible.

## 4. Application of SRP-based information-storage materials

These above-mentioned findings for advanced information encryption and safety not only enrich the library of anti-counterfeiting technologies but also extend the scope of the potential applications of SRPs. SRP-based information-storage

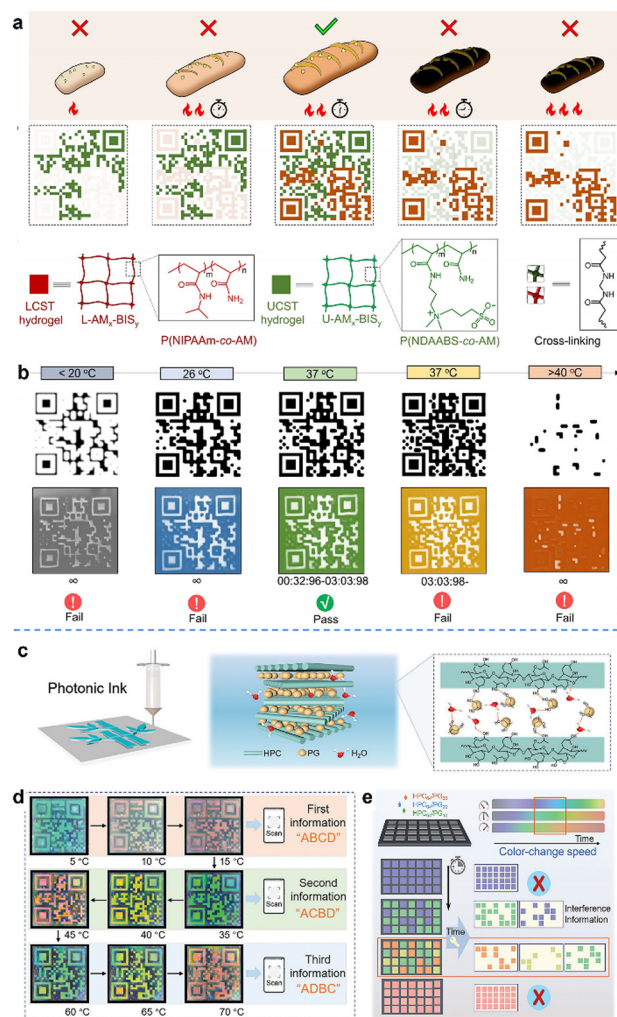


Fig. 19 (a)–(b) Double-lock label based on thermosensitive polymer hydrogels for information camouflage and multi-level encryption.<sup>97</sup> (c) Photonic inks for multilevel information encryption based on hydroxypropyl cellulose (HPC)/propylene glycol (PG) mesophases materials. (d) Temperature-resolved and (e) time-resolved multi-level information encryption and decryption.<sup>98</sup> Reprinted with permission from ref. 97 (Copyright 2022 John Wiley and Sons), and ref. 98 (Copyright 2023 John Wiley and Sons).

systems have been developed with increasing sophistication and are currently employed in several fields due to the advances in material design and manufacturing technologies. In particular, SRPs have been utilized in visualization, medical-biological imaging, intelligent fabric orientation, and criminal investigation fields, and so on. In this section, some potential application scenarios (e.g., logistics and transport, banknote identification, traffic smart display, and information encryption) of multi-mode and multi-level anti-counterfeiting systems based on SRPs are briefly reviewed.

By inseting CNC/PEG-Eu (upper stripe) and CNC/PEG-Tb (lower stripe) materials on banknotes, Zhang *et al.*<sup>68</sup> prepared multi-modal safety labels for advanced quadruple-level anti-counterfeiting. As illustrated in Fig. 20a, if a salesperson in the store is given a brand-new dollar bill with photonic coatings,





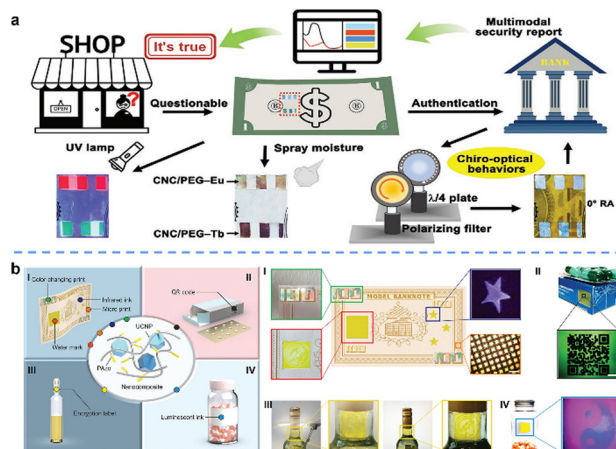


Fig. 20 SRP-based information-storage materials for monetary and product security. (a) CNC-derived photonic composite labels used for banknote anti-counterfeiting.<sup>68</sup> (b) Anti-counterfeiting labels based on PAzo/UCNP nanocomposites.<sup>99</sup> Reprinted with permission from ref. 68 (Copyright 2022 John Wiley and Sons), and ref. 99 (Copyright 2021 John Wiley and Sons).

and is uncertain about the authenticity of the bill, the following four ways can be used to confirm it. First, two strips appear that look finely blue and cyan to the unaided eye when seen in natural light. Second, the CNC/PEG-Eu coating turns yellow and the CNC/PEG-Tb coating turns dark red after spraying moisture. Third, these labels produce brightly fluorescent red and green emissions when exposed to UV light (254 nm). Finally, the neighborhood bank can provide additional proof, in which the chiro-optical behaviors of the banknote are recorded by using a polarizing filter at  $0^\circ$  RA or  $90^\circ$  RA. The ability to easily code multilayer information using light radiation seems interesting, and this anti-counterfeiting tactic is lossless and may be utilized indefinitely.

Similarly, Wu's team<sup>99</sup> integrated four optical signals (structural colors, upconversion luminescence, polarization-dependent patterns, and high-resolution microprint with mesophase textures) in PAzo/UCNP nanocomposites to achieve four anti-counterfeiting functions of a model banknote (Fig. 20b). In addition, the PAzo/UCNP nanocomposites are also appropriate for the anti-counterfeiting protection of a variety of products. For instance, a QR code was created and placed on a pharmaceutical box for checking the authenticity. Moreover, PAzo/UCNP composites could be used to cover the curved surfaces of wine and capsule bottles due to their excellent mechanical properties and processability.

As authentication platforms, dynamic anti-counterfeiting labels can respond to changes in the external environment and play an indicative role, thus having potential application value in logistics transportation. For example, Liu *et al.*<sup>100</sup> fabricated a flexible composite film by embedding luminescent carbon dots (CDs) in oxygen-permeable polyvinylpyrrolidone (PVP), which exhibited ultralong room-temperature phosphorescence (URTP) and could be used as an editable smart logistics label with a time-temperature indicating (TTI) function for

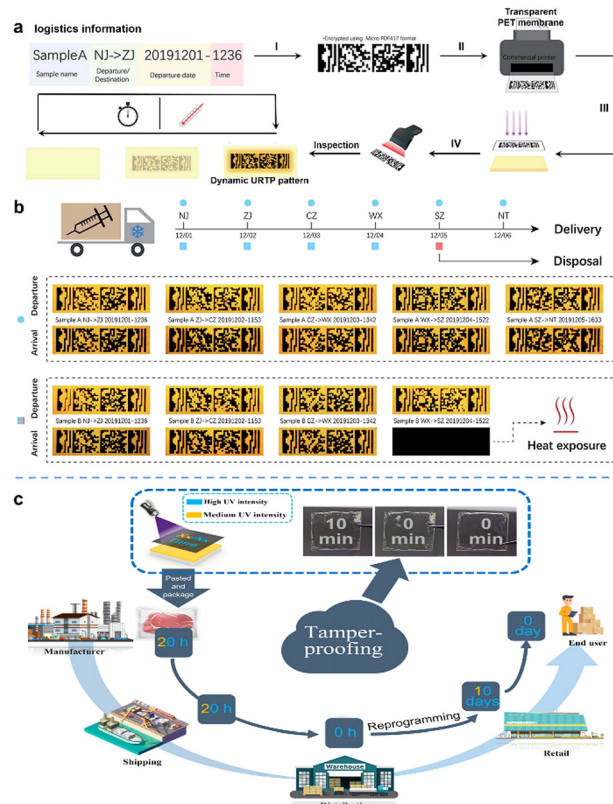


Fig. 21 SRP-based information-storage materials serving as authentication platforms. (a) and (b) CD/PVP film-based smart logistics labels with time-temperature indication functions.<sup>100</sup> (c) S-DSPs for tamper-proofing labels in the supply chain.<sup>74</sup> Reprinted with permission from ref. 100 (Copyright 2021 Royal Society of Chemistry), and ref. 74 (Copyright 2022 Springer).

cold-chain transport (Fig. 21a). As a proof of concept, they created a fictitious 6-step transportation route to show how the changeable logistics-TTI labels might be used. If the cold-chain transport failed, no information could be seen on the label due to the thermal-erasing property, otherwise, all the graphic information could be recognized (Fig. 21b).

Such self-erasing performance could also improve the tamper-proof ability of anti-counterfeiting labels or expiration date labels in the supply chain. As depicted in Fig. 21c, self-erasable dynamic surface patterns (S-DSPs)<sup>55</sup> were created with time-information patterns by regulating the UV intensity and irradiation time, which could be applied to the packaging of fresh goods. During transportation, some patterns (short-term patterns) disappeared within a set amount of time, while others (long-term patterns) did not, and this feature could be used for identifying the authenticity of products. Once the product is affected by other external factors (*e.g.*, light, heat), all the patterns will be affected, proving whether the goods have been replaced or counterfeited. Moreover, 254 nm UV light could be used to completely erase the pattern, while 365 nm UV light could be used to recode a new pattern. These unique S-DSPs for multi-encoded information storage greatly increase the level of encryption.



By taking advantage of the time-dependent self-erasure property, Qu's group constructed a dynamic assembly-induced emissive system based on pyrene derivatives for information encryption.<sup>101</sup> By regulating the solvent composition, the materials could be endowed with different lifetimes of fluorescence color from blue color to yellow, so that multiple information could be presented over a time scale (Fig. 22a). During the whole process of fluorescence discoloration, as well as the solvent evaporation process, only at a specific time would the correct information appear. The letter "C" appeared at 11 min (Fig. 22aII) and the 4D code appeared at 1 min, corresponding to the message "KLAM" (Fig. 22aIII), with both the correct information, while for information that appeared at other time points, either an error message was displayed or a blank message. It is worth mentioning that the new information could be recoded after the solvent had completely evaporated. The instability of the supramolecular emissive system and its controllable fluorescence color can provide new ideas for the design of advanced information encryption materials.

In addition to the above applications, SRP-based information-storage materials can also be employed for smart displays due to

their tunable colors. As demonstrated in Fig. 22b, a retroreflective structural color film (RSCF) that could display both iridescent and non-iridescent structural colors, depending on whether the illumination and viewing angle were coaxial, was constructed and utilized for a nighttime traffic safety application.<sup>102</sup> In a scene with a driver driving at night, a stable colorful traffic signal could be seen at distances of 80, 50, and 30 m, which was ascribed to the fact that the headlights and driver's eyes were roughly parallel to the traffic sign. In contrast, the angle between the pedestrian and the headlights varied with the position of the car, leading to a dynamic changing color signal. Consequently, this kind of signal with unique display performance can serve as a safety warning device.

## 5. Challenges and perspectives

In summary, this review first gave a systematic overview of the latest progress in two categories of SRP-based information-storage systems. One is information in a static state under various modes toward multi-mode anti-counterfeiting systems, and the other is information in a dynamic state containing various optical phenomena toward multi-level information encryption/decryption systems. Then, we focused on the recent practical application of such SRP-based information-storage systems throughout three key areas, including the fields of industry, commerce, and services. In the final section, we summarized the challenges of conventional SRP-based anti-counterfeiting systems' establishment in respect of the materials and technologies designs that still exist today, and correspondingly gave some perspectives for higher-level and more advanced SRP-based information-storage systems.

First and foremost, creating stimulus-responsive polymer materials for multi-mode and multi-level anti-counterfeiting systems continues to be quite tricky. On the one hand, these information-encrypted materials often require high costs and harsh preparation conditions (e.g., sophisticated chemistry or experimental setup).<sup>103,104</sup> Taking advantage of bottom-up preparation methods, such as additive manufacturing, or making full use of other spontaneous physicochemical changes occurring in polymer systems may be effective resolution paths. On the other hand, the vast majority of simply overlaid luminous systems still have mutual interference between different optical channels. Therefore, there is an urgent need to enrich the library of multi-mode and multi-level anti-counterfeiting systems based on SRPs. Exploring appropriate combinations of existing color-alteration units and developing ingenious SRPs systems are both good choices to solve these problems.

Additionally, to meet the current security demands of practical applications, there is still a need for significant efforts to develop SRP-based multi-mode and multi-level anti-counterfeiting systems with additional functions. For instance, self-erasing performance could effectively prevent confidential information from being read by unauthorized persons, and self-healing property could maintain the stability of camouflaged information. What's more, it is quite necessary to create an optimal improved information resolution and high-contrast

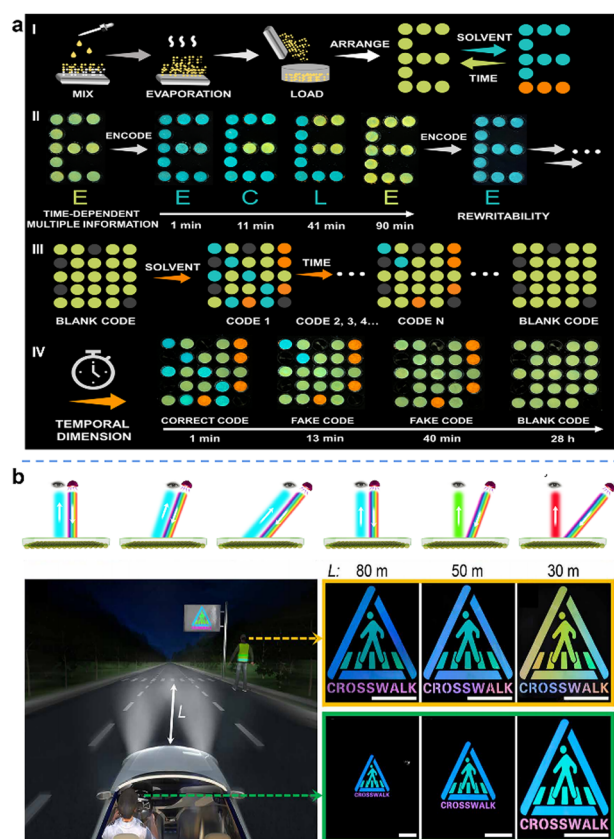


Fig. 22 SRP-based information-storage materials for smart displays. (a) Dynamic assembly-induced multicolor supramolecular system used for information encryption materials with time-dependent security.<sup>101</sup> (b) RSCFs displaying iridescent and non-iridescent structural colors for advertising and nighttime traffic safety.<sup>102</sup> Reprinted with permission from ref. 101 (Copyright 2022 Springer), and ref. 102 (Copyright 2019 American Association for the Advancement of Science).



color display, which would be beneficial for simple identification (read), low cost, convenient visualization, and so on.

The orientation of advanced anti-counterfeiting developments is to closely track the latest achievements of chemical synthetic materials, integrate the technical characteristics of other disciplines, develop encryption compounds with special functions, and develop in the direction of improving their intersection and synthesis. By integrating intelligent anti-counterfeiting systems with bio-inspired actuators/robots, information based on sophisticated interactive information encryption techniques can be realized.<sup>105</sup> Moreover, 3D printing (additive manufacturing),<sup>106,107</sup> screen printing,<sup>108</sup> and other process manufacturing technologies<sup>109,110</sup> could be utilized in the synthesis and preparation of SRP-based anti-counterfeiting materials, jointly promoting the research and application of anti-counterfeiting technology.

With the progressive development of SRP-based information storage toward multi-mode and multi-level anti-counterfeiting materials, such technology would play an increasingly important role in practical applications across a range of domains. Although some progress has been made in the research into SRPs toward advanced information storage (multi-mode anti-counterfeiting and multi-level encryption/decryption), for instance, more enhanced encryption complexity,<sup>111</sup> advanced encryption algorithms,<sup>112</sup> larger information-storage capacities,<sup>113</sup> there still exists considerable difficulties in their future evolution. This review perhaps will inspire further research on developing advanced SRP-based anti-counterfeiting systems that will open new novel avenues to achieve higher-level information security.

## Author contributions

X. Le and Y. Shen proposed the topic of the review. Y. Shen surveyed the literature and compiled the manuscript. X. Le refined the manuscript and provided constructive insight. Y. Shen and Y. Wu edited and proofread the manuscript. X. Le and T. Chen supervised the project. All authors have approved the final version of the manuscript.

## Conflicts of interest

There are no conflicts to declare.

## Acknowledgements

This work was supported by the National Key R&D Program of China (2022YFB3204300), the National Natural Science Foundation of China (52103246), Zhejiang Provincial Natural Science Foundation of China (LQ22E030015), Natural Science Foundation of Ningbo (2023J408, 20221JCGY010301), Ningbo International Cooperation Project (2023H019), the Sino-German Mobility Program (M-0424).

## References

- 1 Y. Wu, X. Chen and W. Wu, *Small*, 2023, **19**, 2206709.
- 2 J. Yan, G. Pan, W. Lin, Z. Tang, J. Zhang, J. Li, W. Li, X. Lin, H. Luo and G. Yi, *Chem. Eng. J.*, 2023, **451**, 138922.
- 3 K. Lou, Z. Hu, H. Zhang, Q. Li and X. Ji, *Adv. Funct. Mater.*, 2022, **32**, 2113274.
- 4 Y. Sun, X. Le, S. Zhou and T. Chen, *Adv. Mater.*, 2022, **34**, 2201262.
- 5 H. Shi, S. Wu, M. Si, S. Wei, G. Lin, H. Liu, W. Xie, W. Lu and T. Chen, *Adv. Mater.*, 2022, **34**, 2107452.
- 6 W. Tian, J. Zhang, J. Yu, J. Wu, J. Zhang, J. He and F. Wang, *Adv. Funct. Mater.*, 2018, **28**, 1703548.
- 7 X. Ji, W. Chen, L. Long, F. Huang and J. L. Sessler, *Chem. Sci.*, 2018, **9**, 7746–7752.
- 8 X. Ji, R. T. Wu, L. Long, X. S. Ke, C. Guo, Y. J. Ghang, V. M. Lynch, F. Huang and J. L. Sessler, *Adv. Mater.*, 2018, **30**, 1705480.
- 9 J. Zhang, H. Shen, X. Liu, X. Yang, S. L. Broman, H. Wang, Q. Li, J. W. Y. Lam, H. Zhang, M. Cacciarini, M. B. Nielsen and B. Z. Tang, *Angew. Chem., Int. Ed.*, 2022, **61**, e202208460.
- 10 H. Peng, S. Bi, M. Ni, X. Xie, Y. Liao, X. Zhou, Z. Xue, J. Zhu, Y. Wei, C. N. Bowman and Y. W. Mai, *J. Am. Chem. Soc.*, 2014, **136**, 8855–8858.
- 11 J. A. Li, L. Zhang, C. Wu, Z. Huang, S. Li, H. Zhang, Q. Yang, Z. Mao, S. Luo, C. Liu, G. Shi and B. Xu, *Angew. Chem., Int. Ed.*, 2023, **62**, e202217284.
- 12 Y. Ding, X. Wang, M. Tang and H. Qiu, *Adv. Sci.*, 2022, **9**, 2103833.
- 13 L. Gu, H. Wu, H. Ma, W. Ye, W. Jia, H. Wang, H. Chen, N. Zhang, D. Wang, C. Qian, Z. An, W. Huang and Y. Zhao, *Nat. Commun.*, 2020, **11**, 944.
- 14 H. Shi, Y. Wu, J. Xu, H. Shi and Z. An, *Small*, 2023, **19**, 2207104.
- 15 H. S. Lim, J.-H. Lee, J. J. Walish and E. L. Thomas, *ACS Nano*, 2012, **6**, 8933–8939.
- 16 S. Wei, Z. Li, W. Lu, H. Liu, J. Zhang, T. Chen and B. Z. Tang, *Angew. Chem., Int. Ed.*, 2021, **60**, 8608–8624.
- 17 J. Bai, Z. Shi and X. Jiang, *Adv. Funct. Mater.*, 2023, **33**, 2301797.
- 18 M. Si, H. Shi, H. Liu, H. Shang, G. Yin, S. Wei, S. Wu, W. Lu and T. Chen, *Mater. Chem. Front.*, 2021, **5**, 5130–5141.
- 19 H. Lu, B. Wu, X. Le, W. Lu, Q. Yang, Q. Liu, J. Zhang and T. Chen, *Adv. Funct. Mater.*, 2022, **32**, 2206912.
- 20 H. Shang, X. Le, M. Si, S. Wu, Y. Peng, F. Shan, S. Wu and T. Chen, *Chem. Eng. J.*, 2022, **429**, 132290.
- 21 K. Hou, D. Guan, H. Li, Y. Sun, Y. Long and K. Song, *Sci. Adv.*, 2021, **7**, eabh3051.
- 22 Z. Li, P. Liu, X. Ji, J. Gong, Y. Hu, W. Wu, X. Wang, H. Q. Peng, R. T. K. Kwok, J. W. Y. Lam, J. Lu and B. Z. Tang, *Adv. Mater.*, 2020, **32**, 1906493.
- 23 Y. Zhang, Y. Su, H. Wu, Z. Wang, C. Wang, Y. Zheng, X. Zheng, L. Gao, Q. Zhou, Y. Yang, X. Chen, C. Yang and Y. Zhao, *J. Am. Chem. Soc.*, 2021, **143**, 13675–13685.
- 24 Z. Gao, Y. Han and F. Wang, *Nat. Commun.*, 2018, **9**, 3977.





- 25 X. Wen, J. Zhang, J. Li, Y. Li, Y. Shi, X. Lu, S. Yang and J. Yu, *Adv. Funct. Mater.*, 2023, 2308973.
- 26 H. Q. Wang, Y. Tang, Z. Y. Huang, F. Z. Wang, P. F. Qiu, X. Zhang, C. H. Li and Q. Li, *Angew. Chem., Int. Ed.*, 2023, e202313728.
- 27 H. Liu, S. Wei, H. Qiu, M. Si, G. Lin, Z. Lei, W. Lu, L. Zhou and T. Chen, *Adv. Funct. Mater.*, 2022, 32, 2108830.
- 28 R. Wang, W. Lu, Y. Zhang, W. Li, W. Wang and T. Chen, *Chin. Chem. Lett.*, 2023, 34, 108086.
- 29 S. Wei, H. Qiu, H. Shi, W. Lu, H. Liu, H. Yan, D. Zhang, J. Zhang, P. Theato, Y. Wei and T. Chen, *ACS Nano*, 2021, 15, 10415–10427.
- 30 S. Wu, H. Shi, S. Wei, H. Shang, W. Xie, X. Chen, W. Lu and T. Chen, *Small*, 2023, 19, 2300191.
- 31 Z. Huang, T. Lan, L. Dai, X. Zhao, Z. Wang, Z. Zhang, B. Li, J. Li, J. Liu, B. Ding, A. K. Geim, H. M. Cheng and B. Liu, *Adv. Mater.*, 2022, 34, 2110464.
- 32 B. Ding, P. Zeng, Z. Huang, L. Dai, T. Lan, H. Xu, Y. Pan, Y. Luo, Q. Yu, H.-M. Cheng and B. Liu, *Nat. Commun.*, 2022, 13, 1212.
- 33 G. H. Lee, T. M. Choi, B. Kim, S. H. Han, J. M. Lee and S. H. Kim, *ACS Nano*, 2017, 11, 11350–11357.
- 34 C. Li, J. Liu, X. Qiu, X. Yang, X. Huang and X. Zhang, *Angew. Chem., Int. Ed.*, 2023, e202313971.
- 35 K. Zhong, J. Li, L. Liu, S. Van Cleuvenbergen, K. Song and K. Clays, *Adv. Mater.*, 2018, 30, 1707246.
- 36 Y. Zhou, C. Lu, Z. Lu, Z. Guo, C. Ye, V. V. Tsukruk and R. Xiong, *Small*, 2023, 19, 2303064.
- 37 M. Qin, M. Sun, R. Bai, Y. Mao, X. Qian, D. Sikka, Y. Zhao, H. J. Qi, Z. Suo and X. He, *Adv. Mater.*, 2018, 30, 1800468.
- 38 E. Yablonovitch, *Phys. Rev. Lett.*, 1987, 58, 2059–2062.
- 39 J. Hou, M. Li and Y. Song, *Angew. Chem., Int. Ed.*, 2018, 57, 2544–2553.
- 40 S. Miao, Y. Wang, L. Sun and Y. Zhao, *Nat. Commun.*, 2022, 13, 4044.
- 41 D. E. McCoy, T. Feo, T. A. Harvey and R. O. Prum, *Nat. Commun.*, 2018, 9, 1.
- 42 M. S. Toivonen, O. D. Onelli, G. Jacucci, V. Lovikka, O. J. Rojas, O. Ikkala and S. Vignolini, *Adv. Mater.*, 2018, 30, 1704050.
- 43 B. Wei, Z. Zhang, D. Yang, D. Ma, Y. Zhang and S. Huang, *ACS Appl. Mater. Interfaces*, 2023, 15, 47350–47358.
- 44 C. Ji, M. Chen and L. Wu, *Adv. Opt. Mater.*, 2022, 10, 2102383.
- 45 Q. Guo, M. Zhang, Z. Tong, S. Zhao, Y. Zhou, Y. Wang, S. Jin, J. Zhang, H. B. Yao, M. Zhu and T. Zhuang, *J. Am. Chem. Soc.*, 2023, 145, 4246–4253.
- 46 Z. Huang, Z. He, B. Ding, H. Tian and X. Ma, *Nat. Commun.*, 2022, 13, 7841.
- 47 S. Lin, Y. Tang, W. Kang, H. K. Bisoyi, J. Guo and Q. Li, *Nat. Commun.*, 2023, 14, 3005.
- 48 C. Dai, Z. Li, Z. Li, Y. Shi, Z. Wang, S. Wan, J. Tang, Y. Zeng and Z. Li, *Adv. Funct. Mater.*, 2023, 33, 2212053.
- 49 B. Guo, M. Wang, D. Zhang, M. Sun, Y. Bi and Y. Zhao, *ACS Appl. Mater. Interfaces*, 2023, 15, 24827–24835.
- 50 Y. X. Hu, X. Hao, L. Xu, X. Xie, B. Xiong, Z. Hu, H. Sun, G. Q. Yin, X. Li, H. Peng and H. B. Yang, *J. Am. Chem. Soc.*, 2020, 142, 6285–6294.
- 51 B. H. Miller, H. Liu and M. Kolle, *Nat. Mater.*, 2022, 21, 1014–1018.
- 52 M. Ni, W. Luo, D. Wang, Y. Zhang, H. Peng, X. Zhou and X. Xie, *ACS Appl. Mater. Interfaces*, 2021, 13, 19159–19167.
- 53 Y. Zhang, J. Wang, L. Wang, R. Fu, L. Sui, H. Song, Y. Hu and S. Lu, *Adv. Mater.*, 2023, 35, 2302536.
- 54 H. Shang, X. Le, Y. Sun, F. Shan, S. Wu, Y. Zheng, D. Li, D. Guo, Q. Liu and T. Chen, *Adv. Opt. Mater.*, 2022, 10, 2200608.
- 55 X. Le, H. Shang, H. Yan, J. Zhang, W. Lu, M. Liu, L. Wang, G. Lu, Q. Xue and T. Chen, *Angew. Chem., Int. Ed.*, 2021, 60, 3640–3646.
- 56 X. Le, H. Shang, S. Wu, J. Zhang, M. Liu, Y. Zheng and T. Chen, *Adv. Funct. Mater.*, 2021, 31, 2108365.
- 57 S. Wei, W. Lu, H. Shi, S. Wu, X. Le, G. Yin, Q. Liu and T. Chen, *Adv. Mater.*, 2023, 35, 2300615.
- 58 Y. Ou, W. Zhou, Z. Zhu, F. Ma, R. Zhou, F. Su, L. Zheng, L. Ma and H. Liang, *Angew. Chem., Int. Ed.*, 2020, 59, 23810–23816.
- 59 Y. Guo, W. Zhu, M. Tao, X. Wu, J. Chen, X. Peng, S. Zheng, Z. Zhao and Z. Cao, *ACS Appl. Mater. Interfaces*, 2022, 14(34), 39384–39395.
- 60 L. R. MacFarlane, H. Shaikh, J. D. Garcia-Hernandez, M. Vespa, T. Fukui and I. Manners, *Nat. Rev. Mater.*, 2020, 6, 7–26.
- 61 S. Wu, H. Shi, W. Lu, S. Wei, H. Shang, H. Liu, M. Si, X. Le, G. Yin, P. Theato and T. Chen, *Angew. Chem., Int. Ed.*, 2021, 60, 21890–21898.
- 62 C. Zheng, S. Tao and B. Yang, *Small Struct.*, 2023, 4, 2200327.
- 63 S. Wu, H. Shi, S. Wei, H. Shang, W. Xie, X. Chen, W. Lu and T. Chen, *Small*, 2023, 19, 2300191.
- 64 N. Gan, H. Shi, Z. An and W. Huang, *Adv. Funct. Mater.*, 2018, 28, 1802657.
- 65 J. Wei, C. Liu, J. Duan, A. Shao, J. Li, J. Li, W. Gu, Z. Li, S. Liu, Y. Ma, W. Huang and Q. Zhao, *Nat. Commun.*, 2023, 14, 627.
- 66 M. Xu, X. Qiu, S. Liang, W. Huang and L. Zhang, *Adv. Opt. Mater.*, 2022, 11, 2201737.
- 67 H. Huang, H. Li, J. Yin, K. Gu, J. Guo and C. Wang, *Adv. Mater.*, 2023, 35, 2211117.
- 68 F. Zhang, Q. Li, C. Wang, D. Wang, M. Song, Z. Li, X. Xue, G. Zhang and G. Qing, *Adv. Funct. Mater.*, 2022, 32, 2204487.
- 69 L. Qin, X. Liu, K. He, G. Yu, H. Yuan, M. Xu, F. Li and Y. Yu, *Nat. Commun.*, 2021, 12, 699.
- 70 Y. Zhao, H. Peng, X. Zhou, Z. Li and X. Xie, *Adv. Sci.*, 2022, 9, 2105903.
- 71 Y. Zhao, X. Zhao, M. D. Li, Z. Li, H. Peng and X. Xie, *Angew. Chem., Int. Ed.*, 2020, 59, 10066–10072.
- 72 M. Xie, F. Xu, L. Zhang, J. Yin and X. Jiang, *ACS Macro Lett.*, 2018, 7, 540–545.
- 73 L. Zhang, J. Bai, T. Ma, J. Yin and X. Jiang, *Macromolecules*, 2022, 55, 6405–6414.
- 74 Z. Fang, X. Lin, Y. Lin, J. Gao, L. Gong, R. Lin, G. Pan, J. Wu, W. Lin, X. Chen and G. Yi, *Nano Res.*, 2022, 16, 634–644.



- 75 T. Ma, T. Li, L. Zhou, X. Ma, J. Yin and X. Jiang, *Nat. Commun.*, 2020, **11**, 1811.
- 76 S. Chen, T. Ma, J. Bai, X. Ma, J. Yin and X. Jiang, *Adv. Sci.*, 2020, **7**, 2002372.
- 77 X. Zhang, C. Qian, Z. Ma, X. Fu, Z. Li, H. Jin, M. Chen, H. Jiang and Z. Ma, *Adv. Sci.*, 2023, **10**, 2206482.
- 78 D. Li, J. Yang, M. Fang, B. Z. Tang and Z. Li, *Sci. Adv.*, 2022, **8**, eabl8392.
- 79 J. Deng, H. Wu, W. Xie, H. Jia, Z. Xia and H. Wang, *ACS Appl. Mater. Interfaces*, 2021, **13**, 39967–39975.
- 80 Y. Su, Y. Zhang, Z. Wang, W. Gao, P. Jia, D. Zhang, C. Yang, Y. Li and Y. Zhao, *Angew. Chem., Int. Ed.*, 2020, **59**, 9967–9971.
- 81 W. C. Xu, C. Liu, S. Liang, D. Zhang, Y. Liu and S. Wu, *Adv. Mater.*, 2022, **34**, 2202150.
- 82 X. Lai, Q. Ren, F. Vogelbacher, W. E. I. Sha, X. Hou, X. Yao, Y. Song and M. Li, *Adv. Mater.*, 2022, **34**, 2107243.
- 83 H. Zhang, Q. Li, Y. Yang, X. Ji and J. L. Sessler, *J. Am. Chem. Soc.*, 2021, **143**, 18635–18642.
- 84 J. Liu, W. Huang, B. Liang, Y. Chen, Y. Liu, X. Zhang, S. Zheng, L. Zhu, S. Feng and W. Huang, *Chem. Mater.*, 2022, **34**, 9492–9502.
- 85 H. Huang, H. Li, X. Shen, K. Gu, J. Guo and C. Wang, *Chem. Eng. J.*, 2022, **429**, 132437.
- 86 J. Fu, J. Feng, B. Shi, Y. Zhou, C. Xue, M. Zhang, Y. Qi, W. Wen and J. Wu, *Chem. Eng. J.*, 2023, **451**, 138240.
- 87 Y. Jiang, J. Ma, Z. Ran, H. Zhong, D. Zhang and N. Hadjichristidis, *Angew. Chem., Int. Ed.*, 2022, **61**, e202208516.
- 88 T. Jiang, Y. F. Zhu, J. C. Zhang, J. Zhu, M. Zhang and J. Qiu, *Adv. Funct. Mater.*, 2019, **29**, 1906068.
- 89 J. Du, L. Sheng, Y. Xu, Q. Chen, C. Gu, M. Li and S. X. Zhang, *Adv. Mater.*, 2021, **33**, 2008055.
- 90 D. Chen, C. Ni, C. Yang, Y. Li, X. Wen, C. W. Frank, T. Xie, H. Ren and Q. Zhao, *Adv. Mater.*, 2023, **35**, 2209956.
- 91 Y. Zhang, X. Le, Y. Jian, W. Lu, J. Zhang and T. Chen, *Adv. Funct. Mater.*, 2019, **29**, 1905514.
- 92 X. Lan, S. Xu, C. Sun, Y. Zheng, B. Wang, G. Shan, Y. Bao, C. Yu and P. Pan, *Small*, 2023, **19**, 2205960.
- 93 G. Su, Z. Li, J. Gong, R. Zhang, R. Dai, Y. Deng and B. Z. Tang, *Adv. Mater.*, 2022, **34**, 2207212.
- 94 H. Xie, Z. Li, J. Gong, L. Hu, P. Alam, X. Ji, Y. Hu, J. H. C. Chau, J. W. Y. Lam, R. T. K. Kwok and B. Z. Tang, *Adv. Mater.*, 2021, **33**, 2105113.
- 95 D. Wang, J. Gong, Y. Xiong, H. Wu, Z. Zhao, D. Wang and B. Z. Tang, *Adv. Funct. Mater.*, 2023, **33**, 2208895.
- 96 S. Xiong, Y. Xiong, D. Wang, Y. Pan, K. Chen, Z. Zhao, D. Wang and B. Z. Tang, *Adv. Mater.*, 2023, **35**, 2301874.
- 97 D. Lou, Y. Sun, J. Li, Y. Zheng, Z. Zhou, J. Yang, C. Pan, Z. Zheng, X. Chen and W. Liu, *Angew. Chem., Int. Ed.*, 2022, **61**, e202117066.
- 98 D. Li, J. M. Wu, Z. H. Liang, L. Y. Li, X. Dong, S. K. Chen, T. Fu, X. L. Wang, Y. Z. Wang and F. Song, *Adv. Sci.*, 2023, **10**, 2206290.
- 99 Y. Liu, S. Liang, C. Yuan, A. Best, M. Kappl, K. Koynov, H. J. Butt and S. Wu, *Adv. Funct. Mater.*, 2021, **31**, 2103908.
- 100 Y. Liu, X. Huang, Z. Niu, D. Wang, H. Gou, Q. Liao, K. Xi, Z. An and X. Jia, *Chem. Sci.*, 2021, **12**, 8199–8206.
- 101 Q. Wang, B. Lin, M. Chen, C. Zhao, H. Tian and D. H. Qu, *Nat. Commun.*, 2022, **13**, 4185.
- 102 W. Fang, J. Zeng, Q. Gan, D. Ji, H. Song, W. Liu, L. Shi and L. Wu, *Sci. Adv.*, 2019, **5**, eaaw8755.
- 103 F. Han, S. Gu, A. Klimas, N. Zhao and S. C. Chen, *Science*, 2022, **378**, 1325–1331.
- 104 Y. F. Yue, M. A. Haque, T. Kurokawa, T. Nakajima and J. P. Gong, *Adv. Mater.*, 2013, **25**, 3106–3110.
- 105 R. Wang, Y. Zhang, W. Lu, B. Wu, S. Wei, S. Wu, W. Wang and T. Chen, *Angew. Chem., Int. Ed.*, 2023, **62**, e202300417.
- 106 Y. Zhang, L. Zhang, C. Zhang, J. Wang, J. Liu, C. Ye, Z. Dong, L. Wu and Y. Song, *Nat. Commun.*, 2022, **13**, 7095.
- 107 J. Liao, C. Ye, J. Guo, C. E. Garciamendez-Mijares, P. Agrawal, X. Kuang, J. O. Japo, Z. Wang, X. Mu, W. Li, T. Ching, L. S. Mille, C. Zhu, X. Zhang, Z. Gu and Y. S. Zhang, *Mater. Today*, 2022, **56**, 29–41.
- 108 B. Lin, Q. Wang, Z. Qi, H. Xu and D.-H. Qu, *Sci. China: Chem.*, 2023, **66**, 1111–1119.
- 109 Y. Gao, M. Wang, Z. Zhang, Y. Liu, J. Zhang, M. Li, H. Ji, W. Zhao, J. Wang and H. Feng, *Adv. Photon. Res.*, 2022, **3**, 2200091.
- 110 D. Guo, Y. Xu, J. Ruan, J. Tong, Y. Li, T. Zhai and Y. Song, *Small*, 2023, **19**, 2208161.
- 111 Y. Ling, J. Liu, Y. Dong, Y. Chen, J. Chen, X. Yu, B. Liang, X. Zhang, W. An, D. Wang, S. Feng and W. Huang, *Adv. Mater.*, 2023, **35**, 2303641.
- 112 Y. Zhang, Z. Yu, H. Qu, S. Guo, J. Yang, S. Zhang, L. Yang, S. Cheng, J. Wang and S. C. Tan, *Adv. Mater.*, 2023, 2208081.
- 113 Y. Yang, Q. Li, H. Zhang, H. Liu, X. Ji and B. Z. Tang, *Adv. Mater.*, 2021, **33**, 2105418.

